

Spectropolarimetry of Supernovae

LIFAN WANG

Texas A&M University: wang@physics.tamu.edu

J. CRAIG WHEELER

The University of Texas at Austin: wheel@astro.as.utexas.edu

Key Words Polarimetry, Stars, Stellar Evolution, Cosmology

Abstract Overwhelming evidence has accumulated in recent years that supernova explosions are intrinsically 3-dimensional phenomena with significant departures from spherical symmetry. We review the evidence derived from spectropolarimetry that has established several key results: virtually all supernovae are significantly aspherical near maximum light; core-collapse supernovae behave differently than thermonuclear (Type Ia) supernovae; the asphericity of core-collapse supernovae is stronger in the inner layers showing that the explosion process itself is strongly aspherical; core-collapse supernovae tend to establish a preferred direction of asymmetry; the asphericity is stronger in the outer layers of thermonuclear supernovae providing constraints on the burning process. We emphasize the utility of the Q/U plane as a diagnostic tool and revisit SN 1987A and SN 1993J in a contemporary context. An axially-symmetric geometry can explain many basic features of core-collapse supernovae, but significant departures from axial symmetry are needed to explain most events. We introduce a spectropolarimetry type to classify the range of behavior observed in polarized supernovae. Understanding asymmetries in supernovae is important for phenomena as diverse as the origins of γ -ray bursts and the

cosmological applications of Type Ia supernovae in studies of the dark energy content of the universe.

CONTENTS

Introduction	3
History	5
<i>Predictions of Supernovae Polarization</i>	5
<i>Early Observational Attempts</i>	6
Introduction to Supernova Spectropolarimetry	8
<i>Stokes Parameters</i>	8
<i>Observational Techniques</i>	9
<i>Interstellar Polarization (ISP)</i>	10
<i>The Dominant Axis</i>	11
<i>Loops in the Q/U Plane</i>	14
<i>Spectropolarimetry Types</i>	16
Core Collapse Supernovae	18
<i>General Trends - Evidence for Bipolar Explosions in the Machine</i>	18
<i>SN 1987A</i>	19
<i>Type II Supernovae</i>	24
<i>Type IIb: SN 1993J and Similar Events</i>	29
<i>Stripped Core (Type Ib and Ic) Supernovae</i>	32
<i>Polarization of High-Velocity SN Ic and GRB-related Events</i>	36
<i>Implications of Polarization for Core Collapse</i>	38
<i>Summary of Core Collapse Spectropolarimetry</i>	40
Thermonuclear Supernovae	40
<i>“Normal” Type Ia</i>	41
<i>Polarization of Subluminous Type Ia</i>	47

<i>The Extremes of Type Ia</i>	47
<i>The Polarization of the Si II 635.5 nm Lines</i>	49
<i>The Implications of Polarization for Thermonuclear Explosions</i>	50
<i>Summary of Type Ia Spectropolarimetry</i>	52
Conclusions	53
Acknowledgments	58

1 Introduction

Supernovae have been studied with modern scientific methods for nearly a century. During this time, it has been traditional to assume that these catastrophic stellar explosions are, for all practical purposes, spherically symmetric. There was no commanding observational need to abandon that simplifying assumption. Now there is.

This article will group supernovae into two major groups: Type Ia supernovae and all the other types that include for example Type II, Type IIb, Type Ib, and Type Ic. (Harkness & Wheeler 1990; Filippenko 1997) [MARGIN COMMENT Type II supernovae show distinct lines of hydrogen. Type I supernovae do not. SN 1987A was a Type II, but the progenitor was a blue supergiant rather than the more common red supergiant. Type Ia supernovae result from exploding white dwarfs, Type Ib and Ic supernovae from core collapse. The progenitors of Type IIb supernovae have a thin hydrogen envelope, $\sim 0.1M_{\odot}$.] Evidence that supernovae may depart a little or even drastically from spherical symmetry has been growing for years. For core collapse, we know that pulsars are somehow “kicked” at birth in a manner that requires a departure from both spherical and up/down symmetry (Lyne & Lorimer 1994). The progenitor star of SN 1987A was

asymmetric as are its surroundings and debris (Wampler et al. 1990; Crotts et al. 1989; Burrows et al. 1995; Wang et al. 2002). The supernova remnant Cassiopeia A shows signs of a jet and counterjet that have punched holes in the expanding shell of debris, and there are numerous other asymmetric supernova remnants (Fesen, 2001; Hwang et al. 2004; Wheeler, Maund & Couch 2008). Each of these observations is well known. The question has been: are they merely incidental or a vital clue to how core-collapse supernovae work?

For Type Ia supernovae (Hillebrandt & Niemeyer 2000) the progenitor white dwarf has long been treated as basically spherically symmetric even though the popular model is that the explosion must take place in a binary system where the white dwarf grows to the critical mass by accretion of mass and, inevitably, angular momentum. There could be asymmetries in this sort of supernova resulting from the the dynamics of the combustion process, the spin of the white dwarf, the stellar orbital motion, a surrounding accretion disk, or the presence of the companion star. As for the case of core-collapse supernovae, this was known, but there was no compelling observational reason to consider departures from spherical symmetry. This, too, is changing.

Our understanding of the shape of supernovae has undergone a revolution in the last decade. The driving force has been a new type of observation: spectropolarimetry. When light scatters through the expanding debris of a supernova, it retains information about the orientation of the scattering layers. Since we cannot spatially resolve the average extragalactic supernova through direct imaging, polarization is the most powerful tool we have to judge the morphology of the ejecta. Spectropolarimetry measures both the overall shape of the emitting region and the shape of regions composed of particular chemical elements. For a

supernova with a typical photospheric radius of 10^{15} cm, the effective spatial resolution attained by polarimetry at 10 Mpc is 10 microarcsec. This is a factor of 100 better resolution than optical interferometers can give us at a small fraction of their cost.

The maturation of spectropolarimetry of supernovae over the last decade occurred in parallel with two other immense revolutions: the supernova/gamma-ray burst connection and the use of Type Ia supernovae to discover the acceleration of the Universe. Understanding that core-collapse supernovae were routinely aspherical developed in parallel with the understanding that long/soft gamma-ray bursts resulted from tightly collimated beams of gamma-rays from some varieties of Type Ic supernovae (Woosley & Bloom 2006). Surely there is a close connection between the asymmetry of “normal” core-collapse supernovae and those that yield gamma-ray bursts. For Type Ia, the knowledge that they are asymmetric is a challenge for their ever more precise use as cosmological tools.

2 History

2.1 Predictions of Supernovae Polarization

Wolstencroft & Kemp (1972) argued that an intrinsic magnetic field dispersed by a supernova explosion might induce optical circular polarization. Shakhovskoi (1976) proposed that electron scattering in an asymmetric, expanding envelope was the most likely source of any intrinsic polarization. Shapiro & Sutherland (1982) did the first quantitative study of polarimetry as an important tool to study the geometry of supernovae. They found that a mixture of scattering and absorption can yield a significantly higher degree of polarization than expected from the classical, pure scattering atmosphere discussed by Chandrasekhar

(1960). More sophisticated models (Höflich 1991) predicted that, for a given axis ratio, the extended atmospheres expected for supernovae would provide even more polarization than a plane-parallel atmosphere.

McCall (1984) argued that lines that form P-Cygni scattering profiles in expanding atmospheres with non-circular isophotes should show a linear polarization greater than that in the continuum. He predicted that the polarization should increase at the absorption minimum as the absorbing material blocked predominantly unpolarized forward scattered flux from the portion of the photosphere along the line of sight. This would increase the relative proportion of polarized flux that scatterered from the asymmetric limb. There is also a tendency for the polarization to decrease at the emission peak because the emitted unpolarized flux will tend to dilute the underlying polarized continuum flux. The result has been characterized as an “inverse P-Cygni” polarization profile across an unblended P-Cygni line in the flux spectrum. [MARGIN COMMENT P-Cygni line profiles form when outflow from a source, the star P-Cygni or a supernova, yields an expanding atmosphere such that there is emission at the rest wavelength of a line from the transverse flow and blue-shifted absorption where the flow expanding toward the observer obscurs the photosphere.]

2.2 Early Observational Attempts

The first reported supernova polarization observations were by Serkowski (1970). Other early attempts were by Shakhovskoi & Efimov (1972), Wolstencroft & Kemp (1972), Lee et al. (1972), and Shakhovskoi (1976). It is not clear that any of these data represented anything but interstellar polarization.

McCall et al. (1984) presented the first spectropolarimetric data on a super-

nova, the Type Ia SN 1983G in NGC 4753 near maximum light. No change in polarization through the P Cygni lines was observed. The polarization at about 2 % was probably due to the interstellar polarization (see §3.3). McCall et al. also looked for circular polarization, but none was detected. McCall (1985) reported observations of the Type Ib SN 1983n close to maximum light and noted that the polarization dipped from about 1.4 % in the continuum to about 0.8 % in the Fe II feature with no change in position angle, strongly suggesting an intrinsic polarization. Unfortunately, the data were never published. Spyromilio and Bailey (1993) obtained spectropolarimetry of the Type Ia SN 1992A 2 weeks and 7 weeks after maximum light. They observed no significant variations across the spectral features.

The first events for which systematic spectropolarimetry was obtained were SN 1987A, an explosion in a rare blue super giant, and SN 1993J, an explosion in a star nearly stripped of its hydrogen envelope. We present a detailed discussion of these events below. These two events illustrated how poor the overall data base of supernova spectropolarimetry was up through the early 1990s.

In 1994 we began a program to obtain spectropolarimetry of as many supernovae as possible that were visible from McDonald Observatory. At the time, as illustrated by this brief history, only a handful of events had been examined at all and there were virtually no statistics. The first few supernovae our group studied (and those in the previous sparse record like SN 1987A and SN 1993J) were classified as “peculiar” in some way, so we did not know whether we were seeing incidental peculiarities or something truly significant.

As data accumulated, however, this uncertainty was removed, and significant new insights were revealed. With more data and better statistics, we identified the

first key trend: the data were bi-modal (Wang et al. 1996). Type Ia supernovae showed little or no polarization signal near and after maximum light (we discuss the prominent pre-maximum polarization below). Supernovae thought to arise by core collapse in massive stars were, by contrast, all significantly polarized. So far every core-collapse supernova for which we or other groups have obtained adequate data has been substantially polarized. Core-collapse supernovae are definitely not spherically symmetric. Table 1 gives a list of supernovae observed with photometric or spectroscopic polarimetry.

3 Introduction to Supernova Spectropolarimetry

3.1 Stokes Parameters

The polarization of an incoming signal can be characterized by its Stokes vector, S , that comprises four components, or Stokes parameters, I , Q , U , and V (Chandrasekhar 1960), where I is the intensity and Q and U measure the linear polarization. The component, V , measures the circular polarization. While a portion of the light from a supernova may be circularly polarized, low flux levels have precluded any serious attempt to measure circular polarization, and it will not be considered here. The Stokes vector has an amplitude and a direction, but since it is related to the intensity, which is the square of the amplitude of the electric vector, it is a quasi-vector for which the directions 0° and 180° are identical.

In general, I is the total flux, \hat{Q} and \hat{U} are differences in flux with the electric vector oscillating in two orthogonal directions on the sky, with \hat{U} representing angles on the sky that are rotated by 45° with respect to those sampled by \hat{Q} . Throughout this review, the normalized Stokes parameters are defined as $Q =$

\hat{Q}/I and $U = \hat{U}/I$. In this way the degree of linear polarization, P , and the polarization angle, θ , are expressed in terms of the Stokes parameters as:

$$P = \frac{\sqrt{\hat{Q}^2 + \hat{U}^2}}{I} = \sqrt{Q^2 + U^2}, \quad (1)$$

and

$$\theta = \frac{1}{2} \arctan \frac{\hat{U}}{\hat{Q}}, \quad (2)$$

or

$$Q = P \cos 2\theta, \quad U = P \sin 2\theta. \quad (3)$$

The astronomical convention is that $\theta = 0^\circ$ points to the North on the sky.

3.2 Observational Techniques

The basic techniques of spectropolarimetry are presented by Miller & Goodrich (1990), Goodrich (1991), del Toro Iniesta (2003), and Patat & Romaniello (2006) (see also van de Hulst 1957). Because polarimetry involves the difference of the ordinary and extraordinary light rays, the per pixel errors are exaggerated compared to those in the total flux spectra and are artificial because each resolution element contains more than one pixel. It is therefore useful to rebin the data into bin sizes comparable to the spectral resolution to reduce the artificial per pixel errors and error correlations. Care must also be taken that estimates of polarization from Equation 1 are not biased to large values by noise (Simmons & Stewart 1985; Wang, Wheeler & Höflich 1997). For a detailed discussion of procedures involved in reducing supernova spectropolarimetry data, see Wang, Wheeler & Höflich (1997), Appendix 1 in Leonard et al. (2001), Leonard & Filippenko (2001), the Appendix in Leonard et al. (2002a), Wang et al. (2003a),

Patat & Romaniello (2006), Maund et al. (2007a) and Maund (2008).

3.3 Interstellar Polarization (ISP)

Polarization introduced by interstellar dust in either the host galaxy or the Milky Way Galaxy can complicate the interpretation of observed polarization. Fortunately, the wavelength dependence of the ISP is well-quantified by observations of Galactic stars (Serkowski et al. 1995; Whitett et al. 1992). The polarization from supernova ejecta is expected to vary across spectral lines and the wavelength dependence may be different. The supernova polarization also varies in time whereas the ISP does not. In principle, these features allow separation of the supernova polarization from the contributions of the ISP.

There is no totally satisfactory method to derive the ISP of supernova polarimetry observationally. Many methods have been proposed, but they have to make assumption about the supernova polarization. Examples of these assumptions are: (1) Certain components of the supernova spectrum, such as the emission peaks of P-Cygni profiles, are not polarized (Trammell et al. 1993; Tran et al. 1997); (2) That the blue end of the supernova spectra is unpolarized because of strong line blended depolarizing lines (Wang et al. 2001). The first method also implicitly assumes a simple axially-symmetric geometry of the ejecta which is often ruled out by the observational data. It is thus often dangerous to derive scientific results assuming that one has an accurate *a priori* knowledge of the (ISP).

If the ISP is significantly larger than the intrinsic polarization of a supernova, the wavelength dependence of the observed polarization can provide estimates of the properties of the dust particles along the line of sight to the supernova. An

estimate of the wavelength at which the ISP reaches maximum can be compared to the that for the Galaxy, around 5500\AA to see if the mean properties of the host dust are similar or different. The ISP due to the dust lanes in Centaurus A was probed by observations of SN 1986G and it was concluded that the size of dust particles are smaller than typical Galactic dust particles (Hough et al. 1987). Recently Wang et al. (2003a) studied the dust properties in NGC 1448 and found the size of dust particles are slightly smaller than their Galactic counterparts, but are nonetheless consist with the properties observed in the Galaxy. Leonard et al. (2002b) observed a highly reddened Type II plateau supernova (see §4.3.1) SN 1999gi in NGC 3184, and found that the polarization efficiency of the dust in NGC 3184 to be much higher than typical Galactic dust. It is certainly important to get more polarization data of highly extinct supernovae as this is a powerful tool to study the elusive properties of extragalactic dust.

3.4 The Dominant Axis

The prominent spectral features of supernovae make it possible to deduce valuable information without accurate estimates of the ISP. Wang et al. (2003a) outlined a method to decompose the observed polarimetry into two components, equivalent to a principle component analysis with two components. In the Q/U plane, the two components correspond to the polarized vectors projected onto the so-called *dominant axis* and onto the axis perpendicular to the dominant axis, which we refer to as the *orthogonal axis*. A dominant axis can often – but not always – be defined from the distribution of the data points on the Q/U plane (Wang et al. 2001). The spectropolarimetry projected to the dominant axis represents global geometric deviations from spherical symmetry, whereas the vector

perpendicular to the dominant axis represents physical deviations from the dominant axis. The coordinates of the new system are given by rotating the original coordinates counterclockwise so that the Q axis overlaps the dominant axis in the new coordinate system and the dominant axis points toward the center of the data cluster on the Q/U plane. The components parallel and perpendicular to the dominant axis are given by

$$P_d = (Q - Q_{ISP}) \cos \alpha + (U - U_{ISP}) \sin \alpha, \quad (4)$$

and

$$P_0 = -(Q - Q_{ISP}) \sin \alpha + (U - U_{ISP}) \cos \alpha, \quad (5)$$

where P_d and P_0 are the polarization components parallel to the dominant axis and orthogonal to that axis, respectively, Q_{ISP} and U_{ISP} are the Stokes parameters of the ISP, $\alpha = 2\theta_d$ is the rotation angle in the Q/U plane and θ_d is the polarization position angle of the dominant axis. An advantage of using these decomposition formulae rather than calculating the degree of polarization as given by Equations 1 and 2 is that the spectral profiles of P_0 and P_d are insensitive to the choice of ISP. A similar procedure producing “rotated Stokes parameters” was employed by Leonard et al. (2001) who calculated a fit to the continuum position angle so that all the continuum polarization falls on the rotated Q. This is equivalent to, but not quite the same technically, as fitting a dominant axis in the Q/U plane. The polarization spectral profiles of the latter decomposition method do not depend on the unknown ISP.

If the supernova ejecta are smooth and axially symmetric, the data points on the Q/U diagram should follow a straight line defining the dominant axis, as expected from theoretical models (Höflich et al. 1996). If the geometry departs significantly from axial symmetry, the data points will show noticeable dispersion

from a straight line, in the direction of the orthogonal axis. These basic situations and their representation in the Q/U plane are shown schematically in Figure 1.

In the top left of Figure 1, we show a smooth, axially symmetric geometric structure with the axis tilted at an arbitrary position angle on the sky and, in general, with respect to the line of sight. For homologous expansion, $v \propto r$, surfaces of constant velocity are planes normal to the line of sight. Viewing at different wavelengths through a line profile corresponds to viewing the geometry along different slices normal to the line of sight. In general, due to the interplay of geometry and optical depth, different wavelengths will register different amplitudes of polarization and hence values of Q and U, but at a fixed angle. The resulting wavelength-dependent polarization amplitude plotted in the Q/U plane will follow a straight line (top right), the dominant axis. A simple rotation of the coordinates would align the rotated Q axis with the line. In this simple example, there would be no contribution along the orthogonal axis corresponding to the rotated U axis.

In the lower left of Figure 1 we schematically illustrate a case for which the axisymmetry is broken, in this case by “clumps” of composition-dependent and hence optical depth- and wavelength-dependent structure. In practice, clumps of high-opacity, absorbing material will block parts of the underlying photosphere. This will induce wavelength-dependent geometry on constant velocity slices even if the underlying photosphere is symmetric and hence imposes no net polarization itself. Clumps blocking an asymmetric photosphere will yield more complex structure, but no difference in principle. In this case, the polarization distribution in the Q/U plane will no longer be along a straight line (lower right). The basic axisymmetric geometry may still be evident in terms of a dominant axis, as

illustrated, but the departure from axial symmetry caused by the “clumping” will yield a finite, and physically significant, distribution along the orthogonal axis. We use this basic phenomenology to define spectropolarimetry types in §3.6.

The decomposition of the polarization components given by Equations 4 and 5 assumes the existence of only two components with fixed axes: an ISP component and only one additional component that is intrinsic to the supernova. This is clearly an oversimplification for some events, for which a more complicated decomposition is needed. A more realistic approach is to assume that the line polarization and continuum polarization have independent geometries and hence that the observed polarization is a combinations of the two.

While there are numerous ways of presenting and analyzing spectropolarimetry data, one clear advantage of displaying the data in the Q/U plane is that it facilitates doing the requisite “vector analysis” by eye. One can immediately and directly see how the amplitude and polarization angle will change with a change in the placement of the always uncertain and frequently controversial ISP. Likewise, the tendency of the data to fall along a single axis, or to depart from a primary axis in loops or other structures, is transparent, completely independent of the placement of the ISP. We will take advantage of this power in the subsequent analysis.

3.5 Loops in the Q/U Plane

In general, the continuum polarization from a supernova provides information about the overall shape of the photosphere, whereas the polarization across spectral lines is more sensitive to small-scale structures in the ejecta. Large-scale gradients in density and composition structure may also affect line polarization,

but such effects are generally saturated for strong lines due to their large optical depth.

If the composition structure is complex, then the degree and angle of polarization may vary significantly across strong spectral lines. The result is to produce “loops” in the Q/U plane. These loops are loci on the Q/U plane that are functions of the wavelength across the line feature and hence functions of the velocity and of the depth of the portion of the structure that contributes to that wavelength. Because the loops represent changes in the amplitude and angle of polarization as a function of wavelength, velocity, and depth, they are specifically evidence for breakdown of axial symmetry. The loops could be caused by composition-dependent clumps or more organized structures that nevertheless break the axial symmetry.

An example of how loops may be formed is given in Figure 2 taken from Kasen et al. (2003), a paper that also has an excellent pedagogical exposition of polarization in supernovae atmospheres. Figure 2 was constructed in the context of the high-velocity calcium feature of Type Ia supernovae (see §5.1.1), but the principles are quite general. In the case illustrated, an edge-on torus surrounds an ellipsoidal photosphere, both expanding homologously. That geometry breaks the axisymmetry. The torus has a strong absorption line that blocks the continuum emission from the photosphere, but the geometry of the blocking region depends on the velocity slices through the structure and hence on the wavelength across the line profile. The resulting locus in the Q/U plane shows a loop that matches the observations (of Type Ia SN 2001el) rather well. Complications that can be envisaged, many of which are discussed by Kasen et al., are an asymmetric photosphere, different geometries for the surrounding shell, and breaking up of

the structure into clumps.

As we shall see in the subsequent discussion, loops in the Q/U plane, with their implied non-axisymmetric structure, are common in both core-collapse and thermonuclear supernovae. These loops represent an important new clue to the physics and the structure of both types of explosion.

3.6 Spectropolarimetry Types

We can classify the spectropolarization characteristics of a supernova according to its distribution in the Q-U diagram. This classification scheme follows directly from the principles outlined in Figures 1 and 2 and is insensitive to the exact value of the ISP. We define the following spectropolarimetric (SP) types:

SP Type N0: This type is characterized by polarization data with no significant deviation from a distribution that is consistent with observational noise. The centroid of the distribution may be offset from zero polarization due to interstellar dust, but there is no measurable supernova polarization. There is no dominant axis.

SP Type N1: This type is characterized by polarization data with no significant elongation in any preferred direction, but for which the data distribution is wider than would be consistent with the observational errors, indicating intrinsic polarization or systematic underestimate of observational error. There is no dominant axis.

SP Type D0: This type is characterized by data that show an elongated ellipse in a Q/U diagram, with the distribution orthogonal to the major axis of the ellipse consistent with observational noise. The locus of the data can be well approximated by fitting a straight line (except in the case of very strong inter-

stellar polarization and very broad wavelength coverage). The position angle of this fitted line defines the dominant axis of the data.

SP Type D1: This type is characterized by data that show an elongated ellipse in a Q/U diagram so that a dominant axis can be identified, but for which a straight line does not provide a satisfactory fit. Significant deviations are found orthogonal to the dominant axis.

SP Type L: Some supernovae show large significant changes in the amplitude and position angle across strong spectral lines. These variations results in prominent loops on the Q/U diagram.

In general, the SP type is deduced from observations at a certain epoch and in a certain wavelength range. The spectropolarimetric properties of supernovae evolve with time, so the SP type as defined here can evolve as well. In addition, different portions of the spectrum may reveal different characteristics. The continuum or a single line could be a D0, while another line could be an L. We have assigned tentative SP types to those supernovae in Table 1 where the data justified it. We also use this classification to discuss individual events in the remainder of this review.

In order to characterize the data, it is critical to correctly estimate both the systematic and the statistical observational errors. In addition to normal spectropolarimetric calibrations such as from observations of polarized and unpolarized standard stars, it is highly advisable to acquire two complete sets of polarization data each night. This allows the errors and stability of the spectropolarimetry to be cross checked with data taken with identical observational setups.

4 Core Collapse Supernovae

4.1 General Trends - Evidence for Bipolar Explosions in the Machine

The single most important conclusion to arise from the study of supernovae spectropolarimetry is that the process of core collapse routinely involves an intrinsically strongly aspherical explosion mechanism that is directed substantially along a single direction in space. Prior to these spectropolarimetric studies, the explosion was assumed to be substantially spherical with any departures from spherical symmetry being due to rather small scale effects of convection or Rayleigh-Taylor instabilities. The evidence for strongly directed explosions has given rise to a new literature of “jet-induced” explosions and variations on that theme (Khokhlov et al. 1999; MacFadyen & Woosley, 1999; Wheeler et al. 2000; Wheeler, Meier & Wilson 2002; Shibata et al. 2003; Maeda & Nomoto 2003; Kotake et al. 2004; Yamada & Sawai 2004; Kifonidis et al. 2006; Obergaulinger et al. 2006; Burrows et al. 2006, 2007; Mezzacappa & Blondin 2007; Moiseenko & Bisnovatyi-Kogan 2007; Komissarov & Barkov 2007; and references therein) and established a strong tie to cosmic long gamma-ray bursts that also involve the collapse of massive stars and highly directed energy output (Woosley & Bloom 2006). Major efforts are now underway to understand the origin of the asymmetry, most plausibly in terms of rotation and magnetic field in the progenitor and newly-formed neutron star (Akiyama & Wheeler 2003; Thompson, Chang & Quataert 2004; Masada et al. 2006; Udzinski & MacFadyen 2007; and references therein). The spectropolarimetry of core-collapse supernovae has thus helped to catalyze a paradigm shift in thinking about the explosion mechanism.

We now recognize that a dominant axis in the polarimetry represents a primarily axisymmetric activity. In the subsequent sections we will summarize in some detail how the data that led to this conclusion were attained, re-visit SN 1987A and SN 1993J in the current context, and attempt to establish a common framework for the interpretation of the data. We will establish that polarization is not a feature of a few odd core-collapse supernovae, but a generic feature of every spectral type. A recent key conclusion is that while a “bipolar” structure is dominant in the geometry of core-collapse supernovae, departures from axisymmetry evidenced by loops in the Q/U plane and other composition-dependent structures are also ubiquitous and must be incorporated in physical models.

4.2 SN 1987A

4.2.1 PHOTOMETRIC POLARIMETRY SN 1987A was the first supernova for which good photometric and spectropolarimetric data were obtained. Although formally a hydrogen-rich Type II supernova, the blue supergiant progenitor and detailed observations of all kinds (Arnett, Bahcall, Kirshner & Woosley 1989; McCray 1993) make this supernova a category unto itself. The polarimetric data on SN 1987A have not been adequately explored. We can view them now in the context of the larger sample of more distant supernovae. The clear conclusion is that more thorough quantitative analysis is warranted, but the basic themes of core-collapse supernovae are reflected here. SN 1987A displayed significant large-scale asymmetry with well-defined principle axes consistent with jet-like flow, but was also marked by departures from axisymmetry. For a complete set of references, see Jeffery (1991a) and Wang et al. (2002).

Some of the early estimates of ISP now appear to have been incorrect and

to have led to incorrect conclusions. With the later and probably more reliable estimate of the ISP, Jeffery (1991a) found that the polarization was small at early times and then grew monotonically for the first month. SN 1987A gave a hint that the inner machine of the explosion was strongly asymmetric, evidence that has proven ubiquitous for core collapse with current, systematic observations. Theoretical models to account for the early behavior of SN 1987A were presented by Méndez et al. (1988), Jeffery (1989), Jeffery (1990), Jeffery (1991b) and Höflich (1991). Models based on the estimate of the ISP by Méndez et al. that implied an early declining value of the polarization need to be reconsidered.

We reproduce in Figure 3 a portion of the data presented by Jeffery (1991a). Figure 3 suggests that around day 140, as the major light curve maximum gave way to the exponential radioactive tail, the polarization jumped to 1.3 – 1.5 % and then slowly dropped back to around 0.2 – 0.4 % by day 200. This jump might be associated with the photosphere receding through the outer hydrogen envelope and revealing the inner core. Whether the polarization of SN 1987A was quite variable in this epoch or some of the data are questionable has yet to be resolved, calling for more study and careful modeling.

A remarkable fact is that the broad-band polarization angle did not waver through this whole evolution, including the possible large spike in the broad-band polarization. The second speckle source, the “mystery spot,” [MARGIN COMMENT The “mystery spot associated with SN 1987A (Meikle et al. 1987; Dotani et al. 1987; Nisenson & Papaliolios 1999) was a small source of luminosity detected in speckle imaging that was nearly as bright as the supernova. No thoroughly satisfactory explanation has been provided.] and the orientation of the late-time HST image of the ejecta at $\theta \sim 16^\circ$ provide another measure of

the orientation (Wang et al. 2002). For compactness, we will refer to this as the “speckle angle” in the subsequent discussion. Scattering from features aligned in this direction would give a plane of polarization with position angle of 106° . Within observational uncertainty, this is very close to the position angle of the continuum polarization. The position angle of the minor axes of the circumstellar rings is also aligned close to the position angle determined from the dominant axis of polarization.

By these measures, SN 1987A “pointed” in a certain direction, a position angle of $\theta \sim 16^\circ$, and maintained that orientation throughout its development (Wang et al. 2002). This requires a large-scale, systematic, directed asymmetry that cannot be accounted for by small-scale convection or turbulence. The continuum polarization probes the geometric structure of the photosphere. The persistent polarization position angle of the dominant axis across a broad wavelength range, and the lack of significant evolution of the polarization position angle strongly argue that the geometry of the photosphere at early and late epochs share the same geometric structure. The data also show that the overall structure of SN 1987A was remarkably axially symmetric from deep inside the oxygen rich zone out to the hydrogen envelope and on to the circumstellar rings. The totality of the data suggests that the angular momentum of the progenitor system played a crucial role in the explosion of SN 1987A (Wang et al. 2002).

4.2.2 SPECTROPOLARIMETRY The first spectropolarimetry of SN 1987A, obtained on 8 March, 1987, was presented by Schwarz & Mundt (1987) and modeled by Jeffery (1987). Broadband polarimetry was also reported by Clocchiatti & Marraco (1988). Subsequent excellent spectropolarimetry of Cropper et al. (1988) confirmed that as data are tracked as a function of wavelength over

spectral features, the polarization angle does sometimes change with wavelength, giving rise to “loops” in the Q/U plane. As explained in §3.5, as wavelength varies over a Doppler-broadened line feature, different depths are sampled in the ejecta, with a given wavelength sampling a velocity “slice” through the ejecta normal to the line of sight. The loops imply that the polarization amplitude and angle are varying along those velocity/depth slices. This means that there must be some substantial departure from axisymmetry in SN 1987A imposed on the overall “pointed” behavior revealed by the photometric polarimetry. As we will now illustrate, this spectropolarimetric behavior gives a rich phenomenology that is ripe for progress in physical understanding of SN 1987A. These loops will give greater insight into the composition-dependent three-dimensional structure of the ejecta and are worth study in much more depth than allowed here. In subsequent sections, we will show that these loops and the implied non-axisymmetry, are not unique to SN 1987A, but common to all core collapse events.

We describe here some of the data of Cropper et al. (1988) corrected for the ISP using the data of Méndez (1990) as parametrized by Jeffery (1991a). As shown in the Q/U diagram of Figure 4 (left panel), when the supernova was about 12 days old, the data in the vicinity of the $H\alpha$ line extend to negative U values corresponding to a position angle $\theta \sim 150^\circ$ with respect to the polarized continuum adjacent to the line. This is similar to, but perhaps significantly different than, the nearly time-independent V-band position angle $\theta \sim 120^\circ$ in Figure 3, and the speckle angle.

Figure 4 (right panel) also shows the dramatically different distribution of the $H\alpha$ polarization in the Q/U plane when the supernova was about 70 days old and approaching maximum brightness. Although the inner, asymmetric core of

the star has yet to be exposed, the variation of polarization across the $H\alpha$ line has changed dramatically. The variation of Q and U with wavelength across the $H\alpha$ line profile now traces out a distinct loop in the Q/U plane. For reference, the $H\alpha$ absorption minimum at 6460 \AA corresponds to the maximum positive Q and U. The distribution at this epoch has little relation to the orientation displayed at the earlier epoch in the left-hand panel of Figure 4. One significant new feature is the distinct loop of green points that fall very close to the speckle angle. Although the photosphere is still in the hydrogen envelope, the hydrogen is clearly, in part, reflecting the dominant asymmetry of the inner regions. A likely cause is the non-spherical distribution of the source of ionization in the form of a “lump” of radioactive nickel and cobalt (Chugai 1992). Departures from the dominant axis lead to loops associated with $H\alpha$. All the complexities displayed here are topics for more in-depth study.

The next epoch presented by Cropper et al. (1988) is on June 3, 1987, about 100 days after the explosion, midway through the decline of the light curve to the radioactive tail and about the time the V-band polarization jumps. A sample of these data is shown in Figure 5. In the vicinity of $H\alpha$ there is again a distinct extension roughly along the speckle angle, but also an interesting loop structure that reflects the non-axisymmetric interplay of the line opacity with the polarized continuum. The absorption minimum at $\sim 6400 \text{ \AA}$ corresponds to the data of most extreme positive Q and U. Significant polarization, primarily along the speckle angle, is shown by $H\alpha$ up to a year after the explosion (Cropper et al. 1988).

The He I $\lambda 5876$ line and surrounding continuum illustrated in the right panel of Figure 5 show remarkable uniformity. The data span $Q = 0$ at $U \sim -1$ with

an exceedingly well-defined dominant axis with position angle, $\theta \sim 4^\circ$. The displacement to negative U can be understood as resulting from the addition of the underlying continuum that adds a wavelength-independent component to the line polarization (Wang et al. 2003b). The polarization angle of this helium feature is not the speckle angle. The simple single-axis behavior of the He line is in stark contrast with that of the $H\alpha$ feature. It is curious that the distinct orientation of the He I line is not imprinted in some way on the H geometry.

While most of the polarization of SN 1987A is intrinsic, the possibility remains that some effects could be induced by dust scattering in the asymmetric environment (Wang & Wheeler 1997)

As in so many other ways, SN 1987A was also a canonical event in terms of its polarimetry. The data deserve a much more thorough quantitative study than has been done, or than we can attempt here, but several key themes emerge. The explosion was definately asymmetric. There is evidence from spectropolarimetry in the continuum and across the $H\alpha$ line for a well-defined physical orientation that corresponds to other evidence for a substantially axially-symmetric structure and “jet-like” flow. On the other hand, there are fascinating and substantial departures from a simple “bi-polar” explosion.

From the perspective of SP types defined in §3.6, the data can be classified as SP Type L with respect to strong P-Cygni lines: $H\alpha$, O I, and Ca II. Across the entire optical wavelength range, the supernova shows an apparent dominant axis which is nearly constant with time and can be classified as SP Type D1. The He I line in Figure 5 can be classified as SP Type D0.

4.3 Type II Supernovae

4.3.1 TYPE II PLATEAU SN 1987A was clearly asymmetric with strong evidence for bi-polar, jet-like flow. This supernova also had obvious peculiarities; its progenitor was a blue supergiant and a binary companion might have been involved. The question remained whether the asymmetries revealed in SN 1987A were peculiar to it, or clues to general processes in core collapse. One means to address this is to examine other Type II supernovae.

Type IIP supernovae explode in red supergiants with extended hydrogen envelopes. Their light curves display a long phase of weeks to months of nearly constant luminosity, called the plateau phase, as the envelope expands and the photosphere recedes by recombination through the envelope. These supernovae are thought to arise in single stars of modest mass, $\sim 10 - 20 M_{\odot}$, and hence to be the most straight forward, “generic” type of core collapse supernova. For that reason, it is especially important to investigate their polarization properties. Spectropolarimetry of Type IIP was reported by Leonard & Filippenko (2001) and Leonard et al. (2002b). Other examples are explored in some detail below.

For Type IIP supernovae, the polarization is usually modest on the plateau phase, but probably not zero. The density structure of the envelope is expected to be nearly spherically symmetric because conservation of angular momentum is likely to lead to slow rotation as the envelope expands after core hydrogen depletion. A likely cause of the early polarization is an asymmetric distribution of radioactive elements that distorts the ionization and excitation structure even though the density structure remains essentially spherically symmetric (Chugai, 1992; Höflich, Khokhlov & Wang, 2001).

One of the best studied examples of a Type II was SN 1999em that displayed a classic, if long-lived, plateau suggesting an especially massive outer hydrogen

envelope (Leonard et al. 2001; Wang et al. 2002b). Observations were obtained from about a week after discovery to about a half-year later. Data for SN 1999em on a Q/U plot are shown in Figure 6. The striking feature is that the data points concentrate on a single line as the wavelength and time vary. The same behavior is well-illustrated in Figure 8 of Leonard et al. (2001) that showed that the polarization of SN 1999em jumped from about 0.2% in the early phases to about 0.5% 160 days later, but with virtually no change in the polarization angle. The constancy of the position angle suggests a well-defined symmetry axis throughout the ejecta and independent of wavelength. Leonard et al. note hints of non-axisymmetry (their Figure 16), but the data is insufficient for detailed study. SN 1999em was a rather typical Type II plateau explosion, yet it demonstrated the key behavior of core-collapse supernovae emphasized in this review: the explosion of SN 1999em was aspherical and aligned along a fixed direction in space. SN 1999em would be classified as a SP Type D0 or D1; a careful study has not been made of the dispersion in the orthogonal direction.

As a Type II plateau supernova continues to expand, the photosphere finally recedes through the hydrogen envelope exposing the ejecta from the heavy-element core. This is accompanied by a sharp drop in luminosity characterizing the end of the plateau phase of the light curve. The plateau phase is typically followed by an exponential decline in luminosity consistent with the decreasing deposition of energy from radioactive decay. The polarization tends to rise rapidly at the end of the plateau phase as the photosphere enters the core ejecta. This was suggested in SN 1987A, in which the polarization jumped from 0.2 to 1.2% at 110 days as the maximum peak gave way to the radioactive decay tail.

This sudden transition was clearly observed in the careful campaign on SN 2004dj

by Leonard et al. (2006), as illustrated in Figure 7. The black points in the left panel give the visual brightness and show the end of the plateau phase and the transition to the exponential tail that is presumed to result from radioactive decay. The red boxes show the dramatic rise in the continuum polarization as the inner core is revealed. The right hand panel in Figure 7 shows the behavior in the Q/U plane from the spike in polarization at 91 days through the subsequent decline as the ejecta thin out and become optically thin to the scattering that induces the polarization. Note the rotation of the polarization angle between the point at 91 days and the point at 128 days by about 30° , after which the angle remains essentially constant.

The origin and evolution of the polarization of SN 2004dj has been discussed and modeled by Chugai et al. (2005) and Chugai (2006) who concludes that a bipolar ejection of radioactive ^{56}Ni with more mass in the near rather than the far hemisphere can account both for the polarization seen in SN 2004dj and the asymmetric profile of the $\text{H}\alpha$ line observed in the nebular phase. Once again, the polarization of SN 2004dj is consistent with a jet-like flow that originates deep in the explosion itself. The rotation of the polarization position angle may suggest that the nickel is broken into clumps (Leonard et al. 2006), that other composition inhomogeneities disrupt the photosphere (Chugai 2006) or that the axis of the “jet” is tilted with respect to another measure of the geometry in the inner regions, perhaps the rotational axis of the core (§4.5.2). The answer could, of course, be a combination of these effects.

4.3.2 TYPE IIn Type IIn supernovae are characterized by hydrogen-rich ejecta with narrow emission lines (Schlegel 1990) that are attributed to emission associated with substantial circumstellar interaction. The differences in the pro-

genitors and their evolution that distinguish these events from classical Type IIP is not clear. Spectropolarimetry can provide useful new information to address the issue.

The first Type IIn with spectropolarimetry was SN 1998S. This event was observed by Leonard et al. (2000) about two weeks before maximum light and by Wang et al. (2001) about 10 and 41 days past maximum light. SN 1998S displayed narrow emission lines characteristic of Type IIn, but also lines characteristic of Wolf-Rayet stars that are not usual for this class. This suggests that SN 1998S had already lost substantial mass from its envelope so that, while very interesting, it may not be representative of all Type IIn. Leonard et al. (2000) favored the interpretation that the broad lines were unpolarized and the narrow lines were polarized. With the benefit of two more epochs of data and the assumption that the ISP does not vary with time, Wang et al. (2001) made a rather different estimate of the ISP. This would give a continuum polarization at the first epoch of $\sim 1.6\%$. This estimate of the ISP also implies that both the broad lines and the narrow lines are polarized in the pre-maximum spectrum with the continuum displaying an essentially constant position angle. Ten days after maximum, the continuum shows a somewhat smaller polarization with a rotation of about 34° compared to the pre-maximum data. The polarization then grows to about 3% while maintaining the same position angle.

A full analysis of the polarization of Type IIn supernovae must also account for the physical state and geometry of the circumstellar medium (Chugai 2001). Hoffman et al. (2007) showed that Type IIn SN 1997eg displayed loops in the Q/U plane over the $H\alpha$ line. This implies that the continuum and line-forming regions had different geometries with different orientations. Hoffman et al. suggest the

that ejecta had an ellipsoidal photosphere and that the circumstellar medium where the hydrogen lines were formed had a flattened disk-like profile. Deeper investigation of this supernova and the polarization of the narrow lines associated with SN 1998S are warranted.

Type IIn supernova usually show a clear dominant axis. They are thus usually SP Type D0 or D1 in the continuum, Some Type IIn show loops across spectral lines Those features would be SP Type L.

4.4 Type IIb: SN 1993J and Similar Events

In the context of asking whether or not the asymmetries of core-collapse supernovae are peculiar to individual events or representative of generic phenomena and whether the asymmetries are associated with the fundamental mechanism of core collapse or peculiarities of the environment, the Type IIb supernovae represent an important test case. [MARGINAL COMMENT The Type IIb events are defined as those that show distinct evidence of hydrogen at early times, but then distinct evidence of helium – similar to a Type Ib – at later epochs. These events are deduced to have lost all but a very thin layer of hydrogen, probably by transfer to a companion. The binary companion to the prototype Type IIb SN 1993J has been specifically identified (Maund et al. 2004).] By examining the Type IIb, one is intrinsically looking closer to the underlying machine of the explosion. Important issues are whether this class of events displays properties similar to other core-collapse supernovae or properties especially characteristic of their class that might be clues to their origin.

4.4.1 SN 1993J [MARGINAL COMMENT SN 1993J showed an initial spike and decline in luminosity attributed to the “fireball” phase as the shock hit

the surface of the star and the shocked material rapidly adiabatically expanded and cooled. This was followed by a secondary peak and a final exponential tail, both presumed to have been powered by radioactive decay. The emergence of the helium lines that mark the class appeared near to the second peak. For an early summary of the polarization data, see Wheeler & Filippenko (1996).]

Doroshenko, Efimov & Shakhovskoi (1995) presented 6 epochs of UBVRI polarimetry of SN 1993J spanning the rise and decline associated with the second peak in the light curve. They found that the U and B data followed a fixed orientation in the Q/U plane, but that the longer wavelength data formed arcs or partial loops with time. Doroshenko et al. suggested that the intrinsic polarization may contain two components that have different orientation and time variability. From the perspective of over a decade later, these remarks seem prescient.

Spectropolarimetry was presented by Trammell, Hines & Wheeler (1993) and by Tran et al. (1997). Both papers assumed that the intrinsic polarization was zero at the peak of the $H\alpha$ line, but differed on their treatment of the underlying continuum. We now recognize that $H\alpha$ can be blended with He I 6678 making the assumption that the $H\alpha$ is unpolarized highly questionable (Maund et al. 2007a). Re-examining the data employing the constraint that the blue end of the spectrum may be substantially de-polarized, the estimate of the ISP by Tran et al. appears to be preferable to that of Trammell et al., although there are questions about the polarization angle assigned by Tran et al. that may affect interpretation of the data. While we believe that the estimate of the ISP by Tran et al. is preferable to that of Trammell et al., we also note that the method used by Tran et al. to subtract the continuum contribution and fit for the ISP can

have significant uncertainties in both the amplitude and angle that they do not assess.

Tran et al. note that they detect the rotation of the position angle across line features in their latest data showing that the emission lines of He I, Fe II, [O I], and H are all intrinsically polarized with position angles that are different from that of the continuum. This also suggests some degree of non-axisymmetric structure. The data for SN 1993J displayed in a Q/U diagram show little evidence for a dominant angle, but real deviation from zero polarization. SN 1993J is classified as an SP Type N1.

4.4.2 SN 2001IG The Type IIb SN 2001ig was observed by Maund et al. (2007a) over multiple epochs. They deduced low intrinsic polarization 13 days after the explosion, $\sim 0.2\%$. This is consistent with a nearly spherical hydrogen-rich envelope. There is a sharp increase in polarization and a rotation of the polarization angle by 40° by 31 days after explosion, after the hydrogen envelope has become optically thin. At this later epoch, the data conform to a dominant axis and would be SP Type D0. The rotation of the position angle shows that the asymmetry of the second epoch was not directly related to that of the first epoch. As illustrated in Figure 8, the most highly polarized lines in SN 1991bg showed wavelength-dependent loop configurations in the Q/U plane (§3.5) so that these lines, especially He I are SP Type L. This demands some non-axisymmetric structure. SN 1991bg was one of the first examples of this loop morphology, a characteristic we have come to recognize as generic in core-collapse explosions. We cite other examples throughout this review.

The polarization properties of SN 2001ig are similar to SN 1993J and SN 1996cb, but not identical. The observing epochs were not the same and the polarization

evolves, so care must be taken in making comparisons. The data suggest that Type IIb supernovae may arise in similar binary systems, but not be so identical that they require identical observer angle, as suggested by Wang et al. (2001). A further implication is that the class of Type IIb supernovae is not simply an artifact of viewing angle. Spectropolarimetry may thus address an important open issue and invites deeper exploration of the nature of the evolution that leads to the progenitors of Type IIb explosions rather than to other types of hydrogen-stripped events. One possibility is that mass transfer in a binary system does not strip the whole hydrogen envelope and that some other process, perhaps a strong stellar wind, is necessary to produce progenitors that are completely stripped of their hydrogen. We explore those sorts of events in the next section.

4.5 Stripped Core (Type Ib and Ic) Supernovae

Type Ib supernovae are classified as those that show strong evidence for helium lines, but scarcely any evidence for hydrogen in the total flux spectra. The total flux spectra of Type Ic supernovae show little evidence for either hydrogen or helium. Among the open issues are why Type Ib and Ic are more devoid of hydrogen than Type IIb, how Type Ic are able to lose much of their helium as well, and which Type Ic are connected to gamma-ray bursts. A goal of continued study of Type Ib and Type Ic supernovae is to seek deeper understanding of the properties of asymmetry that are common to all core collapse events and hence important clues to the physical mechanism of the explosion. Spectropolarimetry may also help to better understand why some progenitors expell virtually all their hydrogen and others, the Type IIb, retain a small amount.

Types Ib and Ic supernovae happen in stars that have already shed nearly all

of their outer hydrogen layers, so they allow us to see deeper into the heart of the exploding star. The trend that these events tend to show more polarization than Type II supernovae was part of our argument (§4.1, Wang et al. 2001) that it was the machinery of the explosion that was aspherical. In this section we explore the data that gave rise to that key conclusion.

4.5.1 SN 1997X The first event that provided hints that Type Ic were more polarized than Type II and hence that the machinery of core collapse was intrinsically strongly asymmetric was the Type Ic SN 1997X (Wang et al. 2001). SN 1997X showed exceptionally high polarization, as much as 7%. Much of this was due to ISP, but the time-dependence showed that there was substantial intrinsic polarization. Wang et al. suggested that the polarization of SN 1997X may have been as high as 4%. There seems to have been a steep drop in polarization in the first 10 days or so, a factor that requires explanation.

SN 1997X displayed little or no evidence of helium lines in its total flux spectrum. That was the basis for its classification as a Type Ic. As illustrated in Figure 9, however, the polarization spectra showed clear spectral features associated with He I $\lambda 5876$ and $\lambda 6678$. The helium absorption features peak at $15,000 \text{ km s}^{-1}$ and the wings reach speeds of $28,000 \text{ km s}^{-1}$. This again shows that spectropolarimetry is a useful tool to reveal important aspects of the progenitor evolution by more tightly constraining the amount and geometry of the helium left in the outer layers of the progenitor. The spectropolarimetry supports arguments that there is a continuum between the Type Ib and the Type Ic, rather than a distinct transition between the two spectral classes. In the Q/U plane, SN 1997X evolves from an SP Type N1 around maximum to an SP Type D1 about a month later.

4.5.2 SN 2005BF SN 2005bf was an especially interesting example of a Type Ib/c supernova. It had a double peaked light curve with a first maximum about 20 days after the explosion and a second, brighter maximum about 20 days later. In addition, it resembled a helium-poor Type Ic in early data, but later developed distinct helium-rich Type Ib features (Tominaga et al. 2005; Folatelli et al. 2006; Parrent et al. 2007). Spectropolarimetry of this event thus gave a chance to look for common aspects of core collapse, clues to the very nature of the Type Ib/c spectral classification, and evidence concerning the special nature of SN 2005bf itself.

Maund et al. (2007b) presented spectropolarimetry SN 2005bf from May 1, 2005, 34 days after the explosion, 18 days after the first peak in the light curve, and 6 days before the second peak when the supernovae was in the Type Ib phase. Although the ISP may have been substantial, intrinsic continuum polarization is still consistent with global asymmetry of order 10%. The data tend to fall along a single locus, suggesting a principal axis and jet-like flow, but also to show considerable scatter around that dominant axis. SN 2005bf showed a distinct loop in the He I $\lambda 5876$ line (Figure 8) adding to the evidence for the ubiquity of such features, perhaps especially in helium, and further suggesting a departure from axisymmetry. Polarization as high as 4% was observed in the absorption components of Ca II H&K and the Ca II IR triplet, rivalling that in SN 1997X. The calcium and helium showed different polarization distributions in the Q/U plane. Iron lines and the prominent O I $\lambda 7774$ line were not polarized (see SN 2002ap for a contrasting case, §4.6). SN 2005bf was SP Type D1 overall and SP Type L in the helium line.

The spectropolarimetry helped to construct a picture of the nature of SN 2005bf

that differed from those already in the literature. The basic premise of Maund et al. was that the progenitor of SN 2005bf comprised a C/O core surrounded by a helium mantle; that is, that the progenitor was structurally that of a Type Ib. The lack of Fe polarization suggested that a nickel jet had not penetrated to the surface. The lack of O I polarization suggested that the photosphere had not receded into the C/O-rich core. This helium star was presumed to have its own axis of symmetry, probably a rotation axis. To that basic picture, Maund et al. added the “tilted-jet.” A possible rationale for this assumption is given by core-collapse models in which the spin axis of the proto-neutron star is de-coupled from the spin axis of the progenitor star (Blondin & Mezzacappa 2007). In the “tilted-jet” model the continuum polarization arises in the aspherical photosphere. The helium mantle contains a solar abundance of calcium. The calcium thus resides primarily in the photosphere and reflects in part the geometry of the photosphere. Some of the calcium is also subject to the asymmetric excitation due to the buried nickel-rich jet that has penetrated the C/O core but not the helium mantle. This gives the calcium a different net polarization angle compared to the photosphere. Unlike the calcium, the helium is only observed due to excitation of the nickel jet. Since it has no photospheric component, it shows yet again another orientation, that of the jet.

Maund et al. suggested that SN 2005bf resembled a Type Ic early on because the photosphere had not yet receded to where the excited helium could be seen. At a later phase, the excited helium could be seen and the supernova resembled a Type Ib. The notion that helium might appear in some events and not others and at different times in different events has long been discussed (Swartz et al. 1993). SN 2005bf showed again that spectropolarimetry is a valuable probe of

the similarities and differences between Type Ib and Type Ic.

While the tilted jet model was designed to qualitatively account for the characteristics of SN 2005bf, its basic features – an asymmetric core that might vary in mass and composition and a tilted jet that carries asymmetric excitation to various depths and at various angles – may help to illuminate other core collapse events. SN 2008D, being observed as this review was completed, may be another example of a SN 2005bf-like event.

4.6 Polarization of High-Velocity SN Ic and GRB-related Events

As remarked in the Introduction, the gamma-ray burst revolution (Woosley & Bloom 2006) unfolded in close parallel to the developments in the polarization of supernovae that we summarize here. There is a strong suggestion that since gamma-ray bursts are the result of jets, spectropolarimetry may also shed light on the supernova/gamma-ray burst connection (Wang & Wheeler 1998). There is a concern that asymmetric explosions could mimic some of the effects of “hypernova” or “high-velocity” activity that have been interpreted as high energy with spherical models (Höflich Wheeler & Wang 1999). Others have argued that large ejecta energy and nickel mass are needed even if the explosion were asymmetric (Maeda et al. 2002).

The most famous example of a high-velocity Type Ic, SN 1998bw, was apparently associated with the gamma-ray burst of April 25, 1998. Much has been written of this event (van Paradijs et al. 2000), a spectacularly bright supernovae and an interestingly dim gamma-ray burst. We will not attempt to summarize that literature here. Spectropolarimetry of SN 1998bw was presented by Patat et al. (2001) that suggested a moderate intrinsic polarization that might have

increased to the red in the earlier data. Few doubt that SN 1998bw was asymmetric. The issue, unresolved, remains what affect asymmetries had on the spectral and photometric properties.

The Type Ic SN 2002ap represented an especially interesting case. This event showed high velocities, but neither a strong relativistic radio source, nor excessive brightness. This event convinced many people that the proper nomenclature for this subset of hydrogen- and helium-deficient supernovae should be “high-velocity Type Ic,” rather than “hypernovae.” Spectropolarimetry was obtained by Kawabata et al (2002), Leonard et al. (2002a) and Wang et al. (2003b) covering about 6 days prior to maximum light to 30 days after maximum. The data were especially interesting and complex, showing a shift in the polarization angle of the continuum and different orientation of position angles for oxygen lines, calcium lines, iron lines, and the continuum. This is strong evidence for non-axisymmetry. SN 2002ap was SP Type D0 in the continuum and SP Type L in strong lines.

The polarized Ca II IR triplet feature appeared later than that of the O I line (Kawabata et al. 2002; Wang et al. 2003b). This behavior is expected if the calcium is primarily resident in the photosphere, but is excited to display an asymmetric geometry only as the ejecta thin out and the outer regions are exposed to the asymmetric excitation of an underlying nickel jet. Wang et al. (2003b) proposed that the jet was still buried in the oxygen mantle in SN 2002ap. A “buried” jet model might then account for the observations of SN 2002ap with the calcium partaking partly of the photospheric geometry and partly of the asymmetric excitation, as also proposed for SN 2005bf (§4.5.2).

SN 2003dh and SN 2006aj were especially interesting as they corresponded to

the counterparts of gamma-ray burst GRB030329 and the X-ray flash XRF060218, respectively. [MARGIN COMMENT X-ray flash events are presumed to be related to gamma-ray bursts, but they show softer radiation outbursts.] A possible polarization of SN 2003dh was reported by Kawabata et al. (2003) at 7000–8000 Å (a region contaminated by sky lines) with a position angle of $\sim 130^\circ$, nearly orthogonal to that of the purported ISP (Kawabata et al.; their Figure 1d). Since the line of sight was closely along the jet of the GRB, presumably a symmetry axis, any polarization would represent non-axisymmetry.

Maund et al. (2007c) reported a single epoch of spectropolarimetry for SN 2006aj obtained about 10 days after the X-ray flash and hence near the estimated maximum of the light curve of the supernova. The polarization is nearly 4% in the blue, making SN 2006aj another rival, like SN 1995bf, to SN 1997X (§4.5.1). This raises the issue as to whether SN 1997X were an XRF. Maund et al. note that their polarization spectrum is consistent with the photometric data of Gorosable et al. (2006) and with the spectropolarimetry of Kawabata et al. (2003) of SN 2003dh, in particular the high polarization of oxygen and calcium. Once again the event is likely to have been observed down the jet axis, and so the polarization is presumed to be due to a breakdown in axisymmetry. SN 2006aj was SP Type L.

4.7 Implications of Polarization for Core Collapse

The fact that the asymmetry of many core-collapse supernovae has a tendency to align in one direction provides an important clue to the engine of the explosion. To do what we see, it seems likely that the mechanism that drives core-collapse supernovae must produce energy and momentum aspherically from the start,

then hold that special orientation long enough for its imprint to be permanently frozen into the expanding matter. Appropriate outflows might be caused by magnetohydrodynamic jets, by accretion flow around the central neutron star, by asymmetric neutrino emission, by magnetoacoustic flux or by some combination of those mechanisms. Another alternative, perhaps intimately related, is that material could be ejected in clumps that block the photosphere in different ways in different lines. It may be that jet-like flows induce clumping so that these effects go together.

The light we see from a supernova comes substantially from the decay of short-lived radioactive elements, ^{56}Ni , ^{56}Co and later ^{44}Ti in the debris. If this material is ejected in an axial fashion, then the overall debris shell could be nearly spherical, while the asymmetric source of illumination leads to a net polarization. This mechanism accounts for the polarization in the early phases of Type IIP supernovae.

By injecting jets of mass and energy up and down along a common axis, typical aspherical configurations emerge. Bow shocks form at the heads of the jets as they plow through the core, and a significant portion of the star's matter bursts through the core along the jet axis. The bow shocks also drive "transverse" shocks and associated flow sideways through the star. These shocks proceed away from the axis, converge toward the star's equator, and collide in the equatorial plane. From there, matter is compressed and ejected in an equatorial torus perpendicular to the jets. Models have shown that sufficiently energetic jets can both cause the explosion of the supernova and imprint asymmetries (Khokhlov et al. 1999). Whether jets of some sort can alone explain the explosion energetics or whether jet-like flow merely supplements the standard neutrino-driven explosion or some

other process remains to be seen. If the jets up and down the symmetry axes are somewhat unequal, they might also account for the runaway velocities of pulsars and more complex flow patterns in the ejecta. There is a need to understand what happens to the dynamics and shape of ejecta if unequal jets break the mirror symmetry.

4.8 Summary of Core Collapse Spectropolarimetry

Every major spectral type of core-collapse supernova has now been sampled with spectropolarimetry. They are all polarized and hence substantially asymmetric. This is a general property of core-collapse, not the peculiarity of single events. While each individual supernova has its own properties, basic themes emerge. The fundamental cause of the asymmetry is deep in the ejecta. It is a generic property of core collapse. The asymmetry is characterized by a dominant polarization angle, the most straightforward explanation of which is directed flow, a jet. Atop this basic structure there are significant, composition-dependent structures that signal generic, large-scale departures from axisymmetry. Any physical model of core collapse must address these realities.

5 Thermonuclear Supernovae

The continuum polarization of Type Ia supernovae tends to be smaller than that for core collapse, but the line polarization can be substantial. The latter is only clearly observed for observations prior to maximum light, so the requisite observations are challenging to acquire. Although the sample is small, a broad range of behavior of Type Ia supernovae has been observed. All show substantial asymmetry.

5.1 “Normal” Type Ia

SN 1996X was the first Type Ia supernova with spectropolarimetry well prior to optical maximum and the first that revealed a polarized component intrinsic to the supernova. Wang, Wheeler & Höflich (1997) presented broadband and spectropolarimetry of SN 1996X about 1 week before and 4 weeks after optical maximum. The Stokes parameters derived from the broadband polarimetry were consistent with zero polarization. The spectropolarimetry showed broad spectral features that were intrinsic to the supernova atmosphere with a rather low polarization $\sim 0.3\%$ that were identifiable only after careful theoretical modeling. The spectral features in the polarized spectrum of SN 1996X were richly structured and showed no strong correlation with the features in the total flux spectrum. Wang et al. noted that because the polarization spectrum is formed at the composition-dependent, and hence wavelength-dependent, last-scattering surface the polarized flux should show a higher degree of wavelength dependence than the multiply-scattered, blended total flux spectrum. Model calculations showed that the polarization could be produced by electron scattering and scattering from blended lines. The models suggested that the polarization was formed at the boundary between the partially burned silicon layers and the inner, iron-peak layers. No other Type Ia with early spectropolarimetry has shown a polarized spectrum quite like SN 1996X. The SP Type of SN 1996X is N1.

Leonard et al. (2005) presented spectropolarimetry of SN 1997dt about 21 days after maximum light. This object did display distinct line polarization in Fe II and Si II, so some of the polarization is intrinsic, but the amount remains uncertain. As we will see below, the polarization of Type Ia supernovae at this later phase tends to be quite low.

5.1.1 SN 2001EL: HIGH-VELOCITY Ca II IR TRIPLET The first detailed, high quality, time-sampled spectropolarimetry of a “core normal” Type Ia (Branch et al. 2006) was obtained for SN 2001el (Wang et al. 2003a). A sample of these data is given in Figure 10. The degree of polarization in the continuum and across spectral lines decreased sharply 10 days after optical maximum, and became undetectable at about 19 days after maximum. Prior to optical maximum, the linear polarization of the continuum was $\sim 0.2 - 0.3\%$ with a constant position angle, showing that SN 2001el had a well-defined axis of symmetry. Significant deviations orthogonal to the dominant axis were seen suggesting that the continuum was SP Type D1. The Si II $\lambda 6355$ line showed a broad loop on the Q/U diagram and is thus of SP Type L across that wavelength range. The polarization was nearly undetectable a week after optical maximum. These data showed that the temporal behavior of Type Ia was just the reverse of core-collapse events. It is the outer layers of Type Ia that are especially asymmetric, not the inner layers.

SN 2001el also gained fame because it was the first Type Ia in which the strong high-velocity, 20,000 - 26,000 km s^{-1} , component of the Ca II IR triplet was observed, a feature separated from the photospheric Ca feature. This high-velocity feature was identified by Hatano et al. (1999) for SN 1994D, but it was much weaker there. The high-velocity Ca II has proven nearly ubiquitous in subsequent studies (Mazzali et al. 2005). This high-velocity component showed much higher polarization than the continuum, $\sim 0.7\%$ versus 0.2 - 0.3%, respectively, and a different position angle. Because the position angle varies across the line, the high-velocity Ca II showed a distinct loop on the Q/U plane making this feature a dramatic example of SP Type L (see Figure 10). The polarization spectrum of SN 2003du obtained by Leonard et al. (2005) 18 days after maximum was

virtually identical to that of SN 2001el at a comparable phase, evidence that this behavior is not isolated to a single rare event. Kasen et al. (2003) showed that the loop in the high-velocity Ca could be accounted for by a clumpy shell or a torus with sufficiently high optical depth (see Figure 3).

Spectropolarimetry of SN 2004S (Chornock & Filippenko 2006) showed that the high velocity component of Ca II IR was not highly polarized although the corresponding position angle was rotated with respect to that of the continuum. The relatively late phase (9 days after maximum light) lends a cautionary note as to whether the low polarization is significant. The behavior of SN 2004S is consistent with that of SN 2001el and shows that it is important to acquire early observations of Type Ia supernovae.

5.1.2 HIGH-VELOCITY PHOTOSPHERIC LINES Another important event was SN 2004dt for which Wang et al. (2006) obtained data about 7 days before maximum and Leonard et al. (2005) did so about 4 days after maximum. Although nominally a normal Type Ia in terms of its light curve, SN 2004dt falls in a subclass of events that show especially high photospheric velocities (as opposed to the high-velocity, separated Ca II IR lines of SN 2001el). This category was discussed by Benetti et al. (2004, 2005) as the High Velocity Gradient (HVG) class and by Branch et al. (2006) as the broad-line class.

SN 2004dt also had a distinct polarization spectrum. The variation of the polarization across some Si II lines approached 2%, putting SN 2004dt among the most highly polarized SN Ia. Unlike SN 2001el, for SN 2004dt the polarization of the Ca II IR features were prominent, but the polarization levels of the lines of Si II were the strongest.

Leonard et al. (2005) also present data on SN 2002bf at about the same

post-maximum time as for their data on SN 2004dt. Ca II is prominent with a polarization of $\sim 2\%$, with the Si II rather modest in the dominant axis. The Si II line shows distinctly in the orthogonal projection, as, perhaps, does a hint of O I. The data on SN 2002bf are thus tantalizingly different than those of SN 2004dt. Other members of the HVG subclass with spectropolarimetry that show strong polarization of the Si II are SN 1997bp and SN 2002bo (Wang et al. 2006).

As illustrated in Figure 11, an especially distinct feature of SN 2004dt was that, in contrast to the strong polarization of Si II (upper left panel), the strong line of O I at 7774\AA showed little polarization signature (lower right panel) along the dominant axis defined by the continuum polarization and by the strong Si II $\lambda 6355$ line. Despite the large evolution in the flux spectrum of SN 2004dt between the premaximum observations of Wang et al. (2006) and the postmaximum observations of Leonard et al. (2005) 11 days later, there was relatively little evolution of the polarized spectrum; the Si II, and Ca II IR triplet remain significantly polarized and the O I is not.

The SP Types across different spectral lines vary for SN 2004dt, as shown in Figure 12. Thanks to the high quality data from the VLT of ESO, the observational errors of SN 2004dt could be determined well enough to enable quantitative studies of the Q/U diagram of SN 2004dt. The Si II lines and the Ca II IR triplet can be classified as SP Type D1 showing distinct dominant axes but with significant dispersion orthogonal to the dominant axis. The Mg II line is classified as SP Type D0 where the Q/U diagram can be well fitted by a straight line. The O I line shows no dominant axis, but with significant dispersion that is too large to be explained by observational errors, and is thus classified as SP Type N1. Note that no significant looping is found for the lines. This is consistent with a low

continuum polarization or only a moderate departure from spherical symmetry of the ejecta. The asymmetry we see in SN 2004dt is perhaps due to lumpy chemical structure with the density of the ejecta more or less spherical, although other possibilities could be considered (Livne 1993; Livne, Asida & Höflich 2005).

The geometrical distributions of different chemical species in SN 2004dt are far from spherical. The degree of polarization in SN 2004dt points to a silicon layer with substantial departure from spherical symmetry. A geometry that would account for the observations is one in which the distribution of oxygen is on average essentially spherically symmetric, but with protrusions of intermediate-mass elements within the oxygen-rich region. The central regions of SN 2004dt are essentially spherical and consist of fully burned iron- group elements. The distribution of magnesium, of SP Type D0, shows a well-defined symmetry axis and rather smooth geometry (see Figure 1) when compared to the distribution of Si and Ca. The prominent dominant axis of SN 2004dt in Si, Ca, and Mg may be the result of an off-centered ignition (Livne 1999; Gamezo et al. 2004; Livne, Asida & Höflich 2005; Röpke, Woosley & Hillebrandt 2007; Plewa, Calder & Lamb 2004; Plewa 2007), or somehow related to the progenitor system.

Leonard et al. (2005) point to the simulations of Travaglio et al. (2004) that had significant unburned C and O as a basis for interpretation. As stressed by Wang et al. (2006), the O has the same velocity profile as the Si in the total flux spectrum, a basic fact that is inconsistent with the model of Travaglio et al., where the silicon remains interior to the unburned oxygen. Wang et al. discuss the inconsistencies of their observations with pure deflagration models that leave substantial unburned C and O.

Another well-studied event of the HVG kind is SN 2006X. This event was

especially marked as the source of the first distinct evidence for a circumstellar medium near a normal Type Ia by Patat et al. (2007). Patat et al. (2008) report 8 epochs of spectropolarimetry of SN 2006X prior to maximum light and one epoch about 40 days later. The polarization of SN 2006X uncorrected for ISP shows a linear decline from about 8% at 4000 Å to about 2% at 8000 Å. This cannot easily be fit with a Serkowski law, implying that the dust around SN 2006X is not of the same constitution as the average in our Galaxy. In the earliest data, 10 days before maximum light, the Ca II IR line is strongly polarized, $\sim 1.5\%$, and the Si II less so, $\sim 0.5\%$. As the peak is approached, the Ca gets less polarized, the Si more so. Especially interesting is that the Ca polarization seems to be stronger at +39 days than it had become at day -1. This may be due to seeing the inner, clumpy, calcium-rich layers. No other SN Ia has been observed at this epoch with this level of S/N ratio, so it is not known if this is a common property, but it may be. More late-time observations are called for. Overall, SN 2006X seems to be intermediate in its polarization properties between SN 2001el and SN 2004dt. Like SN 2004dt, SN 2006X shows little or no polarization of the O I line, less than 0.3%. The continuum shows a reasonably well-defined dominant axis in the Q/U plane, but with significant, and probably real departures. SN 2006X suffers strong interstellar reddening and it is likely that the dust responsible for the reddening is distributed close to the supernova itself (Wang et al. 2007).

It is interesting to point out that all the high-velocity Type Ia show strong polarization, and many of them show strong dust extinction. The interpretation of the polarization data for these supernovae may be complicated by the presence of dust particles around the supernova (Wang, 2005).

5.2 Polarization of Subluminous Type Ia

Another class of Type Ia that can be studied with spectropolarimetry are those in the low-luminosity category, the prototype of which is SN 1991bg. SN 1999by, observed by Howell et al. (2001), is a nice example of a sub-luminous Type Ia. The continuum polarization was substantial (0.3 - 0.8%) and rose toward the red as predicted by models in which the line scattering depolarization is less in the red. The data show a distinct locus in the Q/U plane indicating a favored orientation of the geometry, and hence an SP Type D0. It is not yet clear whether this is a distinguishing characteristic of sub-luminous Type Ia. Howell et al. speculate that the relatively high, well-oriented polarization might be the signature of rapid rotation or binary merger that was a characteristic of sub-luminous events. Howell et al. note that for core normal Type Ia, the photosphere should be near the inner iron-rich layers near maximum light and that these iron lines will affect the spectrum. For a sub-luminous event like SN 1999by near maximum, the photosphere is expected to be still in the silicon layers that are more dominated by continuum scattering.

5.3 The Extremes of Type Ia

5.3.1 THE HYBRID NATURE OF SN 2002IC SN 2002ic showed distinct evidence for narrow-line hydrogen emission similar to Type IIn and indicating strong circumstellar interaction, but with an underlying spectrum that was very similar to a Type Ia (Hamuy et al. 2003). SN 2002ic is thus a very interesting sub-class of Type Ia that have managed, by some circumstance, to explode in a region still rich in hydrogen (see the discussion of SN 2006X above, and the discussion in Gerardy et al. (2004) as to whether the high-velocity Ca II feature represents

a swept up hydrogen shell). Hamuy et al. conclude that the progenitor system contained a massive asymptotic-giant-branch star that lost several solar masses of hydrogen-rich gas before the supernova explosion.

Wang et al. (2004) obtained spectropolarimetry of SN 2002ic nearly a year after the explosion. This is the latest phase of any supernova for which a positive detection of polarization has been made. At this phase, the supernova had become fainter overall, but the $H\alpha$ emission had brightened and broadened dramatically compared to earlier observations. The spectropolarimetry showed spectropolarization properties typical of those of Type IIn supernova, and indicated that the hydrogen-rich matter was highly aspherically distributed. Wang et al. argued that the narrow peak and broad wings of the $H\alpha$ line and the increase in strength of $H\alpha$ with time may be produced by electron scattering in a shocked-heated nebular torus. Chugai & Chevalier (2007) modeled the observed polarization in more detail and concluded that a moderate degree of asymmetry with the major axis about 40-50% longer than the minor axis is sufficient to explain the polarization data. We remark here that the amount of asymmetry deduced by Chugai & Chevalier (2007) represents the minimum level of asphericity required to explain the data, and the level is still very significant. The observations are consistent with about a solar mass of clumpy material extending to $\sim 3 \times 10^{17}$ cm. These observations suggest that the supernova exploded inside a dense, clumpy, disk-like circumstellar environment very reminiscent of a proto-planetary nebula.

5.3.2 SN 2002CX AND SN 2005HK: WEIRD TYPE Ia? SN 2002cx and SN 2005hk were labeled as a “very peculiar” Type Ia showing low peak luminosity, slow decline, high ionization near peak and an unusually low expansion velocity

of only about $6,000 \text{ km s}^{-1}$ (Li et al. 2003; Jha et al. 2006; Chornock et al. 2006; Phillips et al. 2007). The low peak luminosity and slow expansion have been interpreted as possible evidence for an explosion by pure deflagration. Such an explosion is predicted by models to burn less of the white dwarf and to produce less nickel to power the light curve, but in published models this should lead to a significant amount of unburned carbon and oxygen. There is little evidence for that unburned material.

Chornock et al. (2006) presented spectropolarimetry about 4 days before maximum of SN 2005hk. They found that the continuum was polarized about 0.4% in the red with a single axis of symmetry dominating the geometry, but with considerable scatter. They also identified a weak modulation of the polarization of the Fe III line at 5129 \AA . They argued that the fairly large continuum polarization and lack of strong line features are not in keeping with the predictions of the model of Kasen et al. (2004) for a Type Ia viewed “down the hole” carved by a binary companion in the supernova ejecta (Marietta, Burrows & Fryxell 2000). SN 2002cx, SN2005hk, and their kin still defy consistent explanation.

5.4 The Polarization of the Si II 635.5 nm Lines

The Si II 6355 \AA line of Type Ia supernovae is one of the strongest lines in the optical range. Wang, Baade, & Patat (2007) reported polarization data of 17 Type Ia and compared the degree of polarization across the Si II 6355 \AA line to the light curve properties of the supernovae. A general trend was identified that shows that the supernovae with faster light curve decline rate past optical maximum tend to be more highly polarized. The correlation shows a large dispersion due to observational noise, but the correlation appears to be significant. The linear

fit gives $P_{SiII} = 0.48(03) + 1.33(15)(\Delta m_{15} - 1.1)$, where Δm_{15} is the magnitude decline from peak at 15 days after B -band maximum. The supernova showing the highest polarization across the Si II 635.5 nm line is SN 2004dt, which does not follow the linear fit.

Since the continuum polarization is low for all these supernovae, it is clear that the overall structure of Type Ia supernovae must be rather spherical. This is a nice check of using Type Ia as standard candles for cosmological studies.

If we accept Δm_{15} as a measure of the brightness of Type Ia supernovae (Phillips, 1993), and that brighter Type Ia have a larger amount of ^{56}Ni , we can conclude that supernovae with lower polarization have gone through more complete nuclear burning. This may be reasonable since more complete burning tends to destroy more inhomogeneities and thus makes more spherical supernovae.

5.5 The Implications of Polarization for Thermonuclear Explosions

The first polarization models of Type Ia supernovae were presented in Wang et al. (1997). These were based on ellipsoidal variations of one-dimensional thermonuclear combustion models. Kasen et al. (2003) presented models of SN 2001el that explored the polarization properties, especially of the high-velocity Ca II IR triplet that was highly polarized with a different polarization angle than the rest of the spectrum. Kasen et al. investigated the non-axisymmetric geometries necessary to produce “loops” in the Q/U plane. A clumped shell model did an especially good job of accounting for the features of the loop defined by the high-velocity Ca II IR line (see Figure 2 for an example of this sort of calculation), but such models remain phenomenological. A deeper understanding

remains elusive.

Wang et al. (2006) discussed in the context of various models the challenging observations of SN 2004dt that showed polarized Mg, S, and Si, but nearly unpolarized O. This is a puzzle because models predict that these elements should be intermixed in the outer layers of the explosion and hence might be expected to share geometry. One important class of models are deflagration models in which the burning is driven only by subsonic turbulent flames that produce irregular structure, but do not burn the entire C/O white dwarf (Reinecke, Hillebrandt, & Niemeyer (2002); Gamezo et al. 2003; Röpke et al. 2007). Wang et al. concluded that while turbulent deflagration models might produce the observed clumpy composition structure, they have difficulty producing the kinematics of the ejecta, especially the high-velocity yet asymmetric silicon. Another important class of models are the delayed-detonation models (Khokhlov 1991) in which the burning starts as a turbulent, subsonic flame, but there is a presumed transition to a supersonic, shock-driven detonation. These models provide good fits to light curve and spectral data and account for the energetics. Delayed-detonation models burn the outer layers to intermediate mass elements, but are unlikely to generate a turbulent silicon layer as apparently observed in SN 2004dt (Boisseau, et al. 1996; Gamezo et al. 1999). Off-center delayed-detonation models (Livne 1999; Gamezo et al. 2004; Livne, Asida & Höflich 2005; Röpke, Woosley & Hillebrandt 2007) can yield off-center nickel and off-center, clumpy silicon that may contribute to the induction of polarization (Chugai 1992; Höflich 1995a), but there is, as yet, no completely satisfactory model for the polarization of SN 2004dt.

A related possibility is the gravitationally-confined detonation model (Plewa,

Calder & Lamb 2004) or detonating failed deflagration model (Plewa 2007) in which a plume of burned matter floats to the surface and across the surface of the star to converge at the point opposite from where the plume emerges. The resulting rapid compression of the unburned material is proposed to trigger a detonation. This type of model has been explored in some detail by Kasen & Plewa (2007). They generate synthetic broadband optical light curves, near-infrared light curves, color evolution curves, full spectral time series, and spectropolarization of the model, as seen from various viewing angles. They compare the statistical properties of the model to observations and comment on orientation effects that may contribute to photometric and spectroscopic diversity. Kasen & Plewa remark that their model, although based on a particular physical scenario, may be characteristic of a general class of asymmetric models. They made no attempt to compare to a particular supernova, but their total flux spectra do not give a significant O I line and hence their model does not correspond directly to SN 2004dt.

5.6 Summary of Type Ia Spectropolarimetry

Type Ia supernovae are more polarized in the outer layers than the inner. This is an important clue to the nature of their thermonuclear burning. The continuum polarization is low showing that the explosion is nearly spherical, but the line polarization can be very strong. The line polarization may correlate with the velocity measured from absorption line minimum (Leonard et al. 2005). Some Type Ia show significant orientation with a dominant axis, but it is not yet clear whether this correlates with other properties, for instance the light curve decline rate. The future holds great promise to use spectropolarimetry of Type Ia to

explore the asymmetries of the explosion, the nature of the progenitor system, which should be intrinsically asymmetric, and the nature and geometry of the circumstellar medium.

6 Conclusions

Spectropolarimetry of supernovae is still a young field, but a number of basic conclusions can be reached that have important implications for the future of supernova research:

- Spectropolarimetry has now been obtained for every major spectral type of supernova: Type IIP, Type IIIn, Type IIb, Type Ib, Type Ic, and Type Ia of various luminosity classes and peculiarities (Table 1). They are all polarized and hence aspherical in some significant way.
- Presenting the data in the Q/U plane as a function of time, wavelength and especially across individual spectral lines is a powerful way to facilitate analysis of the data.
- Core-collapse supernovae reveal larger asymmetry as observations are made deeper in the ejecta, either as the ejecta thins with expansion or the progenitors have less massive hydrogen envelopes. This is firm evidence that the explosion mechanism itself is strongly asymmetric.
- Type Ia supernovae display modest continuum polarization but very strong line polarization prior to maximum light. The polarization declines after maximum. This is firm evidence that the outer portions of the ejecta are especially significantly aspherical.
- Core-collapse supernovae routinely show evidence for strong alignment of the ejecta in single well-defined directions, suggestive of a jet-like flow.

- Core-collapse supernovae often show a rotation of the position angle with time of $30 - 40^\circ$ that is suggestive of a jet of material emerging at an angle with respect to the rotational axis of inner layers.
- Core-collapse supernovae frequently display loops in the Q/U plane that indicate significant and systematic departures from the predominant axisymmetric structure.
- SN 1987A shows all of the features displayed by core-collapse supernovae: strongly directed flow, but also significant evidence for non-axisymmetric structure. SN 1987A is worthy of in-depth reconsideration in the current context.
- Spectropolarimetry is an especially sensitive tool to study the presence and asymmetry of helium that is excited by non-thermal processes associated with radioactive decay. The helium, in turn, is an important clue to the nature and extent of mass loss from the progenitor, to the relations between Type IIb, Type Ib, and Type Ic supernovae, and to the asymmetric distribution of the radioactive elements.
- Spectropolarimetry of supernovae can reveal information about the properties of the interstellar dust in the host galaxy. Current data suggest that this dust frequently has properties different than dust in the Galaxy.
- Large scale asymmetries in the outermost, high-velocity portions of the ejecta of Type Ia supernovae are not consistent with pure deflagration models, but also not simply explained by delayed-detonation models. This remains a key challenge to models of thermonuclear explosions.

Höflich et al. (1996) argue that to some order the flux spectra of aspherical models can be reproduced by appropriate adjustment of the parameters of spherical models, for instance the radius of the photosphere, the density gradient, or

perhaps some “microturbulence,” so that it is difficult to deduce the geometry from the early time flux spectra of supernovae. Certainly flux spectra are mute to important aspects such as different orientations for different chemical species and “loops” in the Q/U plane. Nebular spectra may be more useful indicators of asymmetry since line profiles can reveal velocity asymmetries and small scale clumping structure, but again, there is no information on the relative orientation of different chemical species.

The totality of the evidence derived from spectropolarimetry of core-collapse supernovae is that the primary driver of asphericity is deep in the explosion process and that the explosion process often “aims” at a certain direction in space. Something resembling jet-like flow is strongly suggested.

As we have summarized here, recent work has revealed that departures from axisymmetry are also ubiquitous in core-collapse supernovae. Much more needs to be done to quantify this significant clue to the physics and dynamics. Two basic means to induce asphericity are from a distortion of the progenitor and a jet-like flow that can induce asphericity in both the density structure and the ionization structure. Jet-like flow is likely to induce significant non-axisymmetric hydrodynamic instabilities: Rayleigh-Taylor, Kelvin-Helmholz, and Richtmyer-Meshkov (Wheeler, Maund & Couch 2008). A non-axisymmetric geometry could also be achieved if the jet-like flow were tilted with respect to the progenitor geometry. There are physical reasons why the rotation axis of a newly-born neutron star and hence, presumably, the jet, could be different than the rotational axis of the progenitor. The jet could also penetrate to different depths in different circumstances, giving considerable variety to the basic picture. In addition, clumps of different density or composition could cause or contribute to the non-

axisymmetry. Ultimately there is also a need to understand the origin of such clumps with the jet being a potential principal source.

It remains true that the characteristics of “high-velocity” Type Ic may be the result of orientation effects in a mildly inhomogeneous set of progenitors, rather than requiring an excessive total energy or luminosity. In the analysis of asymmetric events with spherically symmetric models, it is probably advisable to refer to “isotropic equivalent” energy, luminosity, ejected mass, and nickel mass. The discovery that routine core-collapse supernovae are aspherical and “jet-like” may, in turn, give new insights into more exotic jet-induced events like gamma-ray bursts and X-ray flashes. We desperately need more high quality spectropolarimetry of stripped-core events. This has proved difficult in practice, but the few that have been observed have been exceedingly interesting.

Application of SN II to measurements of the distance scale need to be considered with care since even asymmetric luminosity sources in the plateau phase can give a small direction dependence to the luminosity (Chieffi et al. 2003).

The asymmetries observed in Type Ia may finally yield direct observational evidence that they occur in binary systems, as long assumed, and clues to the combustion mechanism. At this writing, there is no fully acceptable model of the origin of the composition-dependent aspherical structure of Type Ia supernovae, certainly not the possible variation of that structure within the distribution of other observed properties of Type Ia. In particular, neither pure deflagration nor delayed detonation nor gravitationally-confined detonation models fully account for the observations. On the contrary, the spectropolarimetry has offered a new window by which to characterize the nature of the explosion. As the sample grows, we should more deeply understand the nature of the explosion

and how it varies among the normal, luminous, and subluminous Type Ia, and among the high-velocity gradient, broad-line, low-velocity and other sub-genres of the species, such as the hydrogen-rich SN 2002ic and the especially “weird” SN 2002cx. The seemingly ubiquitous, substantially polarized high-velocity Ca II feature is an especially important aspect to explore with spectropolarimetry. Understanding these asymmetries may be necessary to properly interpret future data on cosmologically distant Type Ia’s.

This topic is still in a data-driven phase, but there has been much excellent work to lay the ground for understanding (Jeffery 1989, 1990, 1991b; Höflich 1991; Chugai 1992, 2001, 2006; Kasen et al. 2003; Kasen et al. 2006). Much of the basic understanding of the possible behavior of polarized supernovae, especially of the continuum, has been elucidated in terms of ellipsoidal models (Höflich 1991; Höflich 1995a; Höflich et al. 1996). Prolate models tend to require a larger distortion than oblate models to produce the same net polarization (Höflich et al. 1996). The true geometry may, of course, be some combination of oblate and prolate and more complex than captured easily by ellipsoidal structures.

Exploring more complex structures requires more general models. Monte Carlo radiative transfer models are the most likely to provide the needed generality of the underlying geometry and the capacity to handle the associated radiative transfer with a realistic amount of computer time. Contemporary examples of this are the HYDRA code written by Höflich (2005) and the SEDONA code written by Kasen (see Kasen et al. 2006) which have been applied to a number of problems, especially those associated with Type Ia. These codes treat aspherical geometries, gamma-ray deposition, and line and continuum transfer. They can compute models for the light curves and for the spectral and polarimetric evolution as

observed from arbitrary viewing angles.

There are two ways to approach the analysis of polarization data. One is the solution of the “forward” problem for which a dynamical model is proposed or simulated and the polarimetric evolution is computed to compare with observations. The solution of the “backward” problem consists of proceeding from the observed data to deduce the geometry of the ejecta. In practice, progress will be made by a process of iteration between these two techniques. Codes such as these will play a vital role in this iteration. This phase of supernova polarimetry research is just beginning, but holds great promise as the data base expands.

7 Acknowledgments

The authors are grateful to their fellow members of the VLT spectropolarimetry team for so much of the hard work and insight that made this review possible: PI Dietrich Baade, Peter Höflich, Nando Patat, Alejandro Clocchiatti, and Justyn Maund. Special thanks go to Peter Höflich for his modeling work and early support of the Texas spectropolarimetry program when it was first getting off the ground. JCW is also especially grateful to Justyn Maund for extensive and insightful discussions of supernova polarimetry and related topics and for his help with some of the graphics used here. We also thank Doug Leonard for helpful discussions and for providing specially crafted figures representing his work and Dan Kasen for comments and a key figure. We are indebted to the European Southern Observatory for the generous allocation of observing time for our VLT program and to The Paranal Science Operations staff and the User Support Group in Garching who have gone to considerable effort implement our demanding program. We recognize that accommodating target-of-opportunity

observations in an already busy observing and work schedule often poses a special extra challenge. This work was supported in part by NSF Grant NSF AST 0709181 to LW and NASA Grant NNG04GL00G and NSF Grant AST 0707769 to JCW.

LITERATURE CITED

- Arnett et al.(1989)Arnett, W. D., Bahcall, J. N., Kirshner, R. P., & Woosley, S. E. 1989, *Ann. Rev. Astron. Ap.*, 27, 629
- Benetti et al. (2004)Benetti, S. et al. 2004, *MNRAS*, 348, 261
- Benetti et al.(2005)Benetti, S., et al. 2005, *Ap. J.*, 623, 1011
- Blondin & Mezzacappa(2007)Blondin, J. M., & Mezzacappa, A. 2007, *Nature*, 445, 58
- Boisseau, Wheeler, Oran, & Khokhlov(1996)Boisseau, J. R., Wheeler, J. C., Oran, E. S., & Khokhlov, A. M. 1996, *ApJl*, 471, L99
- Branch et al.(2006)Branch, D., et al. 2006, *Pub. Astr. Soc. Pac.*, 118, 560
- Burrows et al.(1995)Burrows C. J., et al. 1995, *Ap. J.*, 452, 680.
- Burrows et al.(2007)Burrows, A., Dessart, L., Livne, E., Ott, C. D., & Murphy, J. 2007, *Ap. J.*, 664, 416
- Chandrasekhar(1960)Chandrasekhar, S. 1960, New York: Dover
- Chieffi et al.(2003)Chieffi, A., Domínguez, I., Höflich, P., Limongi, M., & Straniero, O. 2003, *Mon. Not. Royal. Soc.*, 345, 111
- Chornock et al.(2006)Chornock, R., Filippenko, A. V., Branch, D., Foley, R. J., Jha, S., & Li, W. 2006, *PASP*, 118, 722
- Chugai(2001)Chugai, N. N. 2001, *Mon. Not. Royal. Soc.*, 326, 1448
- Chugai (1992)Chugai, N. N. 1992, *SvAL*, 18, 168

- Chugai(2006)Chugai, N. N. 2006, *Astronomy Letters*, 32, 739
- Chugai & Chevalier(2007)Chugai, N. N., & Chevalier, R. A. 2007, *Ap. J.*, 657, 378
- Chugai et al.(2005)Chugai, N. N., Fabrika, S. N., Sholukhova, O. N., Goranskij, V. P., Abolmasov, P. K., & Vlasjuk, V. V. 2005, *Astronomy Letters*, 31, 792
- Clocchiatti & Marraco(1988)Clocchiatti, A., & Marraco, H. G. 1988, *Astron. & Astroph.*, 197, L1
- Cropper et al.(1988)Cropper, M., Bailey, J., McCowage, J., Cannon, R. D., Couch, W. J., Walsh, J. R., Straede, J. O., & Freeman, F. 1988, *MNRAS*, 231, 695
- Crotts et al.(1989)Crotts, A. P. S., Kunkel, W. E., & McCarthy, P. J. 1989, *Ap. J. Lett.*, 347, L61
- del Toro Iniesta(2003)del Toro Iniesta, J. C. 2003, *Cambridge:Cambridge University Press*
- Doroshenko et al.(1995)Doroshenko, V. T., Efimov, Y. S., & Shakhovskoi, N. M. 1995, *Astronomy Letters*, 21, 513
- Dotani et al.(1987)Dotani, T., Hayashida, K., Inoue, H., Itoh, M. & Koyama, K. 1987, *Nature*, 330, 230
- Fesen(2001)Fesen, R. A. 2001 *Ap. J. Supp.*, 133, 161
- Filippenko(1997)Filippenko, A. V. 1997, *Ann. Rev. Astron. Ap.*, 35, 309
- Folatelli et al.(2006)Folatelli, G., et al. 2006, *Ap. J.*, 641, 1039
- Gamezo, V. N., Wheeler, J. C., Khokhlov, A. M., & Oran, E. S. (1999)*Ap. J.*, 512, 827
- Gamezo et al.(2003)Gamezo, V. N., Khokhlov, A. M., Oran, E. S., Chtchelkova, A. Y., & Rosenberg, R. O. 2003, *Science*, 299, 77

- Gamezo et al.(2004)Gamezo, V. N., Khokhlov, A. M., & Oran, E. S. 2004, PHRvL, 92, 102
- Gerardy et al. (2004)Gerardy, C. L., Höflich, P., Fesen, R. A., Marion, G. H., Nomoto, K., Quimby, R., Schaefer, B. E., Wang, L., & Wheeler, J. C. 2004, Ap. J., 607, 391
- Goodrich(1991)Goodrich, R. W. 1991, Pub. Astr. Soc. Pac., 103, 1314
- Gorosabel et al.(2006)Gorosabel, J., et al. 2006, Astron. & Astroph., 459, L33
- Hamuy et al.(2003)Hamuy, M., et al. 2003, Nature, 424, 651
- Hanuschik et al.(1989)Hanuschik, R. W., Thimm, G., & Seidensticker, K. J. 1989, A&A, 220, 153
- Harkness & Wheeler(1990)Harkness, R. P., & Wheeler, J. C. 1990, Supernovae, p. 1 - 29, 1
- Hatano et al.(1999)Hatano, K., Branch, D., Fisher, A., Baron, E., & Filippenko, A. V. 1999, Ap. J., 525, 881
- Hillebrandt & Niemeyer(2000)Hillebrandt, W., & Niemeyer, J. C. 2000, Ann. Rev. Astron. Ap., 38, 191
- Hoffman et al.(2007)Hoffman, J. L., Leonard, D. C., Chornock, R., Filippenko, A. V., Barth, A. J., & Matheson, T. 2007, ArXiv e-prints, 709, arXiv:0709.3258
- Höflich(1991)Höflich P. 1991 å, 246, 481
- Höflich(1995a)Höflich, P. 1995a, Ap. J., 440, 821
- Höflich (1995b)Höflich, P. 1995b, Ap. J., 443, 89
- Höflich & Khokhlov(1996)Höflich, P. & Khokhlov, A. 1996, Ap. J., 457, 500
- Höflich et al.(1996)Höflich, P., Wheeler, J. C., Hines, D. C., & Trammell, S. R. 1996, Ap. J., 459, 307
- Höflich et al.(1999)Höflich, P., Wheeler, J. C., & Wang, L. 1999, Ap. J., 521, 179

- Höflich, Khokhlov & Wang(2001)Höflich, P., Khokhlov, A., & Wang, L. 2001, in
Proc. of the 20th Texas Symposium on Relativistic Astrophysics, eds. J. C.
Wheeler & H. Martel (New York: AIP), 459
- Höflich et al.(2002)Höflich, P., Gerardy, C. L., Fesen, R. A., & Sakai, S. 2002,
ApJ, 568, 791
- Höflich(2005)Höflich, P. 2005, Ap. and Space. Sci., 298, 87
- Hough et al.(1987)Hough, J. H., Bailey, J. A., Rouse, M. F., & Whittet, D. C. B.
1987, Mon. Not. Royal. Soc., 227, 1P
- Howell et al.(2001)Howell, D. A., Höflich, P., Wang, L., & Wheeler, J. C. 2001,
ApJ, 556, 302
- Hwang et al.(2004)Hwang, U., et al. 2004, Ap. J. Lett., 615, L117
- Jeffery(1987)Jeffery, D. J. 1987, Nature, 329, 419
- Jeffrey(1989)Jeffrey, D. J. 1989, Ap. J. Supp., 71, 951
- Jeffery(1990)Jeffery, D. J. 1990, Ap. J., 352, 267
- Jeffery(1991a)Jeffery, D. J. 1991a, Ap. J. Supp., 77, 405
- Jeffrey (1991b)Jeffrey, D. J. 1991b, ApJ, 375, 264
- Jha et al.(2006)Jha, S., Branch, D., Chornock, R., Foley, R. J., Li, W., Swift,
B. J., Casebeer, D., & Filippenko, A. V. 2006, Astrophys. Journal, 132, 189
- Kasen et al.(2003)Kasen, D., et al. 2003, ApJ, 593, 788
- Kasen et al.(2004)Kasen, D., Nugent, P., Thomas, R. C., & Wang, L. 2004, ApJ,
610, 876
- Kasen et al.(2006)Kasen, D., Thomas, R. C., & Nugent, P. 2006, Ap. J., 651, 366
- Kasen & Plewa(2007)Kasen, D., & Plewa, T. 2007, Ap. J., 662, 459
- Kawabata et al.(2002)Kawabata, K. S., et al. 2002, ApJl, 580, L39
- Kawabata et al.(2003)Kawabata, K. S., et al. 2003, ApJl, 593, L19

- Khokhlov & Höflich(2001)Khokhlov, A., & Höflich, P. 2001, in AIP Conf. Proc. No. 556, Explosive Phenomena in Astrophysical Compact Objects, eds. H.-Y, Chang, C.-H., Lee, & M. Rho (New York: AIP), 301
- Khokhlov et al.(1999)Khokhlov, A. M., Höflich, P. A., Oran, E. S., Wheeler, J. C., Wang, L., & Chtchelkanova, A. Y. 1999, ApJl, 524, L107
- Kifonidis et al.(2006)Kifonidis, K., Plewa, T., Scheck, L., Janka, H.-T., Müller, E. 2006, Astron. & Astroph., 453, 661
- Komissarov & Barkov(2007)Komissarov, S. S., & Barkov, M. V. 2007, Mon. Not. Royal. Soc., 382, 1029
- Kotake et al.(2004)Kotake, K., Sawai, H., Yamada, S., & Sato, K. 2004, Ap. J., 608, 391 D. C. B., & Hough, J. H. 1996, Ap. J., 472, 755
- Lee et al.(1972)Lee, T. A., Wamsteker, W., Wisniewski, W. Z., & Wdowiak, T. J. 1972, ApJl, 177, L59
- Leibundgut(2001)Leibundgut, B. 2001, Ann. Rev. Astron. Ap., 39, 67
- Leonard et al.(2000)Leonard, D. C., Filippenko, A. V., Barth, A. J., & Matheson, T. 2000, ApJ, 536, 239
- Leonard & Filippenko(2001)Leonard, D. C. & Filippenko, A. V. 2001, PASP, 113, 920
- Leonard et al. (2001)Leonard, D. C., Filippenko, A. V., Ardila, D. R., & Brotherton, M. S. 2001, ApJ, 553, 861
- Leonard et al.(2002a)Leonard, D. C., Filippenko, A. V., Chornock, R., & Foley, R. J. 2002a, PASP, 114, 1333
- Leonard et al.(2002b)Leonard, D. C., et al. 2002b, Astron. J., 124, 2490
- Leonard et al.(2005)Leonard, D. C., Li, W., Filippenko, A. V., Foley, R. J., & Chornock, R. 2005, Ap. J., 632, 450

- Leonard et al.(2006)Leonard, D. C., et al. 2006, *Nature*, 440, 505
- Leonard & Filippenko(2005)Leonard, D. C., & Filippenko, A. V. 2005, in *ASP Conference Series Proceedings: "Supernovae as Cosmological Lighthouses"*, Eds. M. M. Turatto, S. Benetti, L. Zampieri, & W. Shea (San Francisco: ASP), 342, 330
- Li et al.(2003)Li, W., et al. 2003, *PASP*, 115, 453
- Livne (1999)Livne, E. 1999, *ApJ* 527, L97
- Livne et al.(2005)Livne, E., Asida, S. M., Höflich, P. 2005, *ApJ*, 632, 443
- Livne(1993)Livne E. 1993, *ApJ* 406, L17
- Lyne & Lorimer(1994)Lyne, A. G., & Lorimer, D. R. 1994, *Nature*, 369, 127
- MacFadyen & Woosley(1999)MacFadyen, A. I., & Woosley, S. E. 1999, *Ap. J.*, 524, 262
- Maeda & Nomoto(2003)Maeda, K., & Nomoto, K. 2003, *ApJ*, 598, 1163
- Maeda et al.(2002)Maeda, K., Nakamura, T., Nomoto, K., Mazzali, P. A., Patat, F., & Hachisu, I. 2002, *ApJ*, 565, 405
- Marietta, Burrows & Fryxell(2000)Marietta, E., Burrows, A., & Fryxell, B. 2000, *ApJs*, 128, 615
- Mazzali et al.(2005)Mazzali, P. A., et al. 2005, *Ap. J. Lett.*, 623, L37
- Maund(2008)Maund, J.R. *Astron. & Astroph.*, in press
- Maund et al.(2007)Maund, J. R., Wheeler, J. C., Patat, F., Wang, L., Baade, D., Höflich, P. A. 2007, *Ap. J.*, 671, 1944
- Maund et al.(2007)Maund, J. R., Wheeler, J. C., Patat, F., Baade, D., Wang, L., Höflich, P. 2007, *Mon. Not. Royal. Soc.*, 381, 201
- Maund et al.(2007)Maund, J. R., Wheeler, J. C., Patat, F., Baade, D., Wang, L., Höflich, P. 2007, *Astron. & Astroph.*, 475, L1

- Maund et al.(2008)Maund, J.R., Wheeler, J.C., Patat, F., Wang, L., Baade, D., & Höflich, P.A. 2008, in preparation for Ap. J.
- Masada et al.(2006)Masada, Y., Sano, T., & Takabe, H. 2006, Ap. J., 641, 447
- McCall et al.(1984)McCall, M. L., Reid, N., Bessell, M. S., & Wickramasinghe, D. 1984, MNRAS, 210, 839
- McCall(1984)McCall, M. L. 1984, MNRAS, 210, 829
- McCall(1985)McCall, M. L. 1985, LNP Vol. 224: Supernovae as Distance Indicators, 224, 48
- McCray(1993)McCray, R. 1993, Ann. Rev. Astron. Ap., 31, 175
- Meikle, Matcher & Morgon(1987)Meikle, W. P. S., Matcher, S. J. & Morgan, B. L. 1987, Nature, 329, 608
- Méndez et al.(1988)Méndez, M., Clocchiatti, A., Benvenuto, O. G., Feinstein, C., & Marraco, H. G. 1988, Ap. J., 334, 295
- Méndez(1990)Méndez, M. 1990, private communication to D. Jeffery
- Miller & Goodrich(1990)Miller, J. S., & Goodrich, R. W. 1990, Ap. J., 355, 456
- Moiseenko & Bisnovaty-Kogan(2007)Moiseenko, S. G., & Bisnovaty-Kogan, G. S. 2007, Ap. and Space. Sci., 311, 191
- Nisenson & Papaliolios(1999)Nisenson, P. & Papaliolios, C. 1999 Ap. J., 518, L29
- Obergaulinger et al.(2006)Obergaulinger, M., Aloy, M. A., Dimmelmeier, H., Müller, E. 2006, Astron. & Astroph., 457, 20
- Parrent et al.(2007)Parrent, J., et al. 2007, Pub. Astr. Soc. Pac., 119, 135
- Patat et al.(2001)Patat, F. et al. 2001, ApJ, 555, 900
- Patat & Romaniello(2006)Patat, F., & Romaniello, M. 2006, Pub. Astr. Soc. Pac., 118, 146 Science, 317, 924
- Patat et al.(2007)Patat, F., et al. 2007,

- Patat et al.(2008)Patat, F., et al. 2008, *Astron. & Astroph.*, in press
- Phillips(1993)Phillips, M. M. 1993, *Ap. J. Lett.*, 413, L105
- Phillips et al.(2007)Phillips, M. M., et al. 2007, *Pub. Astr. Soc. Pac.*, 119, 360
- Plewa et al.(2004)Plewa, T., Calder, A. C., & Lamb, D. Q. 2004, *ApJ*, 612, L37
- Plewa(2007)Plewa, T. 2007, *Ap. J.*, 657, 942 & Hu, J. 1999, *Astron. J.*, 117, 736
- Reineke, Hillebrandt, & Niemeyer(2002)Reinecke, M., Hillebrandt, W., & Niemeyer, J. C. 2002, *A&A*, 391, 1167
- Riess et al.(1998)Riess, A. G. et al. 1998, *Astrophys. Journal*, 116, 1009
- Röpke et al.(2007)Röpke, F. K., Hillebrandt, W., Schmidt, W., Niemeyer, J. C., Blinnikov, S. I., & Mazzali, P. A. 2007, *Ap. J.*, 668, 1132
- Röpke, Woosley & Hillebrandt(2007)Röpke, F. K., Woosley, S. E., & Hillebrandt, W. 2007, *Ap. J.*, 660, 1344
- Schlegel(1990)Schlegel, E. M. 1990, *Mon. Not. Royal. Soc.*, 244, 269
- Schwarz & Mundt(1987)Schwarz, H. E. & Mundt, R. 1987, *Astron. & Astroph.*, 177, L4
- Serkowski(1970)Serkowski, K. 1970, *ApJ*, 160, 1083
- Serkowski, Mathewson & Ford(1975)Serkowski, K., Mathewson, D. L., & Ford, V. L. 1975, *ApJ*, 196, 261
- Shakhovskoi & Efimov(1972)Shakhovskoi, N. M., & Efimov, Y. S. 1972, *Soviet Astronomy*, 16, 7
- Shakhovskoi(1976)Shakhovskoi, N. M. 1976, *Soviet Astronomy Letters*, 2, 107
- Shapiro & Sutherland(1982)Shapiro, P. R., & Sutherland, P. G. 1982, *ApJ*, 263, 902
- Simmons & Stewart(1985)Simmons, J. F. L., & Stewart, B. G. 1985, *Astron. & Astroph.*, 142, 100

- Shibata et al.(2003)Shibata, M., Karino, S., Eriguchi, Y. 2003, Mon. Not. Royal. Soc., 343, 619
- Spyromilio & Bailey(1993)Spyromilio, J., & Bailey, J. 1993, Proceedings of the Astronomical Society of Australia, 10, 263
- Swartz et al.(1993)Swartz, D. A., Filippenko, A. V., Nomoto, K., & Wheeler, J. C. 1993, ApJ, 411, 313
- Thompson et al.(2004)Thompson, T. A., Chang, P., & Quataert, E. 2004, Ap. J., 611, 380
- Tominaga et al.(2005)Tominaga, N., et al. 2005, Ap. J. Lett., 633, L97
- Trammell, Hines & Wheeler(1993)Trammell, S. R., Hines, D. C., & Wheeler, J. C. 1993, ApJl, 414, L21
- Tran et al.(1997)Tran, H. D., Filippenko, A. V., Schmidt, G. D., Bjorkman, K. S., Jannuzi, B. T., & Smith, P. S. 1997, PASP, 109, 489
- Travaglio et al.(2004)Travaglio, C., Hillebrandt, W., Reinecke, M., & Thielemann, F.-K. 2004, Astron. & Astroph., 425, 1029
- Van de Hulst(1957)Van de Hulst, H. C. 1957, New York: Wiley
- Uzdensky & MacFadyen(2007)Uzdensky, D. A., & MacFadyen, A. I. 2007, Ap. J., 669, 546
- van Paradijs et al.(2000)van Paradijs, J., Kouveliotou, C., & Wijers, R. A. M. J. 2000, Ann. Rev. Astron. Ap., 38, 37
- Wampler et al.(1990)Wampler, E. J., Wang, L., Baade, D., Banse, K., D’Odorico, S., Gouiffes, C., & Tarenghi, M. 1990, Ap. J. Lett., 362, L13
- Wang(2005)Wang, L. 2005, Ap. J. Lett., 635, L1
- Wang et al.(1996)Wang, L., Wheeler, J. C., Li, Z., & Clocchiatti, A. 1996, ApJ, 467, 435

- Wang, Wheeler, & Höflich(1997)Wang, L., Wheeler, J. C., & Höflich, P. 1997, ApJl, 476, L27
- Wang & Wheeler(1998)Wang, L., & Wheeler, J. C. 1998, ApJl, 504, L87
- Wang et al. (2001)Wang, L., Howell, D. A., Höflich, P., & Wheeler, J. C. 2001, ApJ, 550, 1030
- Wang et al.(2002)Wang, L., Wheeler, J. C., Höflich, P., Khokhlov, A., Baade, D., Branch, D., Challis, P., Filippenko, A. V., Fransson, C., Garnavich, P., Kirshner, R. P., Lundqvist, P., McCray, R., Panagia, N., Pun, C. S. J., Phillips, M. M., Sonneborn, G., & Suntzeff, N. B. 2002b, ApJ, 579, 671
- Wang et al.(2003a)Wang, L., Baade, D., Höflich, P., Khokhlov, A., Wheeler, J. C., Kasen, D., Nugent, P. E., Perlmutter, S., Fransson, C., & Lundqvist, P. 2003a, ApJ, 591, 1110
- Wang et al.(2003b)Wang, L., Baade, D., Höflich, P., & Wheeler, J. C. 2003b, ApJ, 592, 457
- Wang et al. 2004Wang, L., Baade, D., Höflich, P., Wheeler, J. C., Kawabata, K., & Nomoto, K. 2004, ApJ, 604, L53
- Wang et al.(2006)Wang, L., Baade, D., Höflich, P., Wheeler, J. C., Kawabata, K., Khokhlov, A., Nomoto, K., & Patat, F. 2006, ApJ, 653, 490
- Wang et al.(2007)Wang, L., Baade, D., & Patat, F. 2007, Science, 315, 212
- Wheeler & Filippenko(1996)Wheeler, J. C., & Filippenko, A. V. 1996, IAU Colloq. 145: Supernovae and Supernova Remnants, 241
- Wheeler(2000)Wheeler, J. C. 2000, American Institute of Physics Conference Series, 522, 445
- Wheeler, Maund, & Couch(2008)Wheeler, J. C., Maund, J. R., & Couch, S. M. 2008, Ap. J., in press

Wheeler et al.(2002)Wheeler, J. C., Meier, D. L., & Wilson, J. R. 2002, Ap. J.,
568, 807

Wheeler et al.(2000)Wheeler, J. C., Yi, I., Höflich, P., & Wang, L. 2000, Ap. J.,
537, 810

Whittet et al.(1992)Whittet, D. C. B., Martin, P. G., Hough, J. H., Rouse, M. F.,
Bailey, J. A., & Axon, D. J. 1992, Ap. J., 386, 562

Wolstencroft & Kemp(1972)Wolstencroft, R. D., & Kemp, J. C. 1972, Nature,
238, 452

Woosley & Bloom(2006)Woosley, S. E., & Bloom, J. S. 2006, Ann. Rev. Astron.
Ap., 44, 507

Yamada & Sawai(2004)Yamada, S. & Sawai, H. 2004, Ap. J., 608, 907

Table 1: Supernovae with Polarimetric Data

Supernova	Host Galaxy	Type	Photometric (P)	No. of Epochs: epoch ¹	References
			Spectroscopic (S)	(SP Type)	
1968L	M83 (NGC 5236)	IIP	P (undetermined)	1	1
1970G	M101 (NGC 5457)	IIl	P	1	2
1972E	NGC 7723	Ia	P (undetermined)	3	3
1975N	NGC 7723	Ia	P? (undetermined)	2: 0, 34	4
1981B	NGC4536	IA	P (undetermined)	1: 56	5
1983G	NGC 4753	Ia	S? (undetermined)	1: -2	6
1983N	NGC 5236 (M83)	Ib	S	1: 1	6
1986G	NGC5128	Ia	S	2: -9, -8	7
1987A	LMC	IIpec	P, S	many	8
1992A	NGC 1380	Ia	S (undetermined)	1: 12 (N)	9
1993J	M81	IIb	P, S	17 (D1, L): -15, -14, -11 +2(x2), +8, +9, +10, +12 +23, +26 plus 6 photometry	10
1994D	NGC 4526	Ia	P (undetermined)	1: -10	11
1994Y	NGC 5371	IIIn	P	1: >180 (D0?)	11
1994ae	NGC 3370	Ia	P (undetermined)	1: >30 (N0)	11
1995D	NGC 2962	Ia	P (undetermined)	2: 14 (N0), 41 (N0)	11
1995H	NGC 3526	II	P	1 > 33	11
1995V	NGC 1087	II	P?	n	12
1996B	NGC 4357	IIb	S	1?	13
1996W	...	II	S?	n	12
1996X	NGC 5061	Ia	S	1 (N1)	14
1996cb	NGC 3510	IIb	S	n (D1, L)	15
1997X	NGC 4691	Ic	S	2: ~5, ~30 (D1, L1)	15
1997Y	...	Ia	S (undetermined)	n (N0)	12
1997bp	NGC 4680	Ia	S?	n (D0)	12

Table 1: Continued

Supernova	Host Galaxy	Type	Photometric (P)	No. of Epochs: epoch ²	References
			Spectroscopic (S)	(SP Type)	
1997bq	NGC 3147	Ia	S (undetermined)	1 (D1)	12
1997br	...	Ia	S (undetermined)	1 (D1)	12
1997dq	NGC 3810	Ib	S	1 (D1)	16
1997ds	MCG -01-57-007	II	S	1 (D1)	17
1997dt	NGC 7448	Ia	S	1 (N1)	18
1997ef	UGC 4107	Ib/c (high velocity)	S (undetermined)	2? (N1)	19
1997eg	NGC 5012	IIn	S	3: 16, 44, 93 post discovery (D1)	20
1997ei	NGC 3963	Ic	S	1	12
1998A	IC 2627	II	S	1	17
1998S	NGC 3877	IIn	S	3: -14, 10, 41 (D)	21
1998T	NGC 3690	Ib	S	1	16
1998bw	-	Ic (pec)	S	2: -6, 10 (N)	22
1999by	NGC 2841	Ia (subluminous)	S	3: -2, -1, 0 (D1)	23
1999em	NGC 1637	IIP	P, S	7: 7, 10, 40, 49, 73 (D), 159, 163 (after discovery)	24
1999gi	NGC 3184	II	S	1 (D, L)	17
2001V	NGC 3987	Ia	S	1 (D1, N)	25
2001X	NGC 5921	IIP	S	1 (D)	25
2001bb	??	Ic	S	1(D1)	25
2001dh	MCG -6-44-26	II P?	S	2 (D, L)	25
2001dm	??	Ia	S	1 (N, D)	25
2001du	NGC 1365	IIP	S	1 (N, D)	25
2001el	NGC 1448	Ia	S	5: -4 (D1, L), +2 (D1, L) +11 (D), +20 (N1), +41 (N1)	26
2001lig	NGC 7424	I Ib	S	3:+13 (D, L), +31 (D, L), +256	27

Table 1: Continued

Supernova	Host Galaxy	Type	Photometric (P)	No. of Epochs: epoch ³	References
			Spectroscopic (S)	(SP Type)	
2002ap	M74 NGC 628	Ic (HV)	S	S: -6 (, L), -2 (N, L), 0 () +1(x2) (D, L), +2, +3(x2), +5, +26, +27, +29	28
2002bo	NGC 3190	Ia	S	2 (L)	25
2002el	NGC 6986	Ia	S	1 (D)	25
2002fk	NGC 1309	Ia	S	2 (D)	25
2002bf	??	Ia	S	1 (N)	18
2002ic	??	Ia (pec)	S	5: 221 (D1), 232 (D1) 253 (D1), 255 (D1), 315 (D1)	29
2003B	NGC 1097	II	S	1 (D)	25
2003L	NGC 3506	Ic	S	1 (D)	25
2003W	UGC 5234	Ia	S	1 (D)	25
2003bu	??	Ic	S	2 (D)	25
2003dh	a104450+213117	Ic (HV)	S	2: 15 (N), 16 (N)	30
2003du	UGC 9391	Ia	S	1 (D)	18
2003ed	NGC 5303	IIb	S	1	38
2003ee	??	IIIn	S	1 (D1)	25
2003eh	??	Ia	S	1(N1)	25
2003gd	M74 NGC 628	IIP	S	1 (D)	25
2003gf	MCG -04-52-026	Ic	S	1	38
2003hh	??	Ia	S	2 (D1)	25
2003hv	NGC 1201	Ia	S	1 (D)	25
2003hx	NGC 2076	Ia	S	1 (D)	25
2003hy	IC 5145	IIIn	S	1 (D1)	25
2004S	MCG-05-16-021	Ia	S	1 (D)	31
2004dj	NGC 2403	II	S	1 (D)	32

Table 1: Continued

Supernova	Host Galaxy	Type	Photometric (P)	No. of Epochs: epoch ⁴	References
			Spectroscopic (S)	(SP Type)	
2004dk	NGC 6118	Ib	S	1 (D)	25
2004dt	NGC 799	Ia	S	2 -7 (D1, L), +4 (D1, L)	33
2004br	NGC 4493	Ia (pec)	S	1 (N1)	25
2004dk	NGC 6118	Ib	S	1 (D1)	25
2004ef	UGC 12158	Ia	S	1 (D1)	25
2004eo	NGC 6928	Ia	S	1 (D1)	25
2005bf	MCG+00-27-005	Ib/c	S	1: -6 (wrt 2nd max) (D1, L)	34
2005cf	MCG -1-39-3	Ia	S	1 (N1)	25
2005de	UGC 11097	Ia	S	2 (N1)	25
2005df	NGC 1559	Ia	S	2 (D1)	25
2005el	NGC 1819	Ia	S	1 (D1)	25
2005hk	UGC 272,	Ia (pec)	S	3: -4 (D1), 0 (D1) , +14 (D1)	35
2005ke	NGC 1371	Ia	S	2 (D1)	25
2006X	NGC 4321	Ia	S	9: -10 (D1, L), -8 (D1, L) -7 (D1, L), -6 (D1, L), -3 (D1, L) -2 (D1, L), -1 (D1, L), +39 (N1)	36
2006aj	a032140+165203	Ib/c (XRF)	P, S	9: -7 (N1), -6 (N1), -5 (N1) -4 (N1), 0 (N1), +3 (N1) +8 (N1), +29 (N1), 300?? (N0)	37
2006bc	NGC 2397	II	S	1 (D)	25
2006be	IC 4582	II	S	1 (D)	25
2007af	NGC 5584	Ia	S	2	25
2007fb	UGC 12859	Ia	S	4	25
2007hj	NGC 7461	Ia	S	3	25
2007if	anon	Ia	S	5	25
2007it	UGC 10553	II	S	3	25
2007le	NGC 7721	Ia	S	3	25
2008D	NGC 27720	Ib/c (pec)	S	2 (D1)	25

References - (1) Wood & Andrews (1974); Serkowski (1970); (2) Shakhovskoi & Efimov (1972); (3) Wolstoncraft & Kemp (1972), Lee et al. (1972), Shakhovskoi (1976); (4) Shakhovskoi (1976); (5) Shapiro & Sutherland (1982); (6) McCall et al. (1984), McCall (1985); (7) Hough et al. (1987); (8) Cropper et al. (1988), Méndez et al. (1988); (9) Spyromilio & Bailey (1993); (10) Trammel, Hines, & Wheeler (1993), Doroshenko, Efimov & Shakhovskoi (1995), Tran et al. (1997) ; (11) Wang et al. (1996); (12) Wheeler (2000); (13) mentioned in Wang et al. (2001); (14) Wang, Wheeler & Höflich (1997); (15) Wang et al. (2001); (16) Leonard, Filippenko, & Matheson (2000); (17) Leonard & Filippenko (2001); (18) Leonard et al. (2005); (19) Leonard et al. (2000); Wheeler (2000); (20) Leonard et al. (2000); (21) Leonard et al. (2000); Wang et al. (2001); (22) Patat et al. (2001); (23) Howell et al. (2001); (24) Leonard et al. (2001); Wang et al. (2001); (25) unpublished; (26) Wang et al. (2003a); (27) Maund et al. (2007c); (28) Kawabata et al. (2002), Leonard et al. (2002), Wang et al. (2003); (29) Wang et al. (2004), Kawabata et al. unpublished; (30) Kawabata et al. (2003); (31) Chornock & Filippenko (2006); (32) Leonard et al (2006); (33) Leonard et al. (2005), Wang et al. (2006); (34) Maund et al. (2007a); (35) Chornock et al. (2006), Maund et al. (2007d) ; (36) Patat et al. in prep; (37) Gorosabel et al. (2006), Mazzali et al. (2007), Maund et al. (2007c); (38) Leonard & Filippenko (2005)

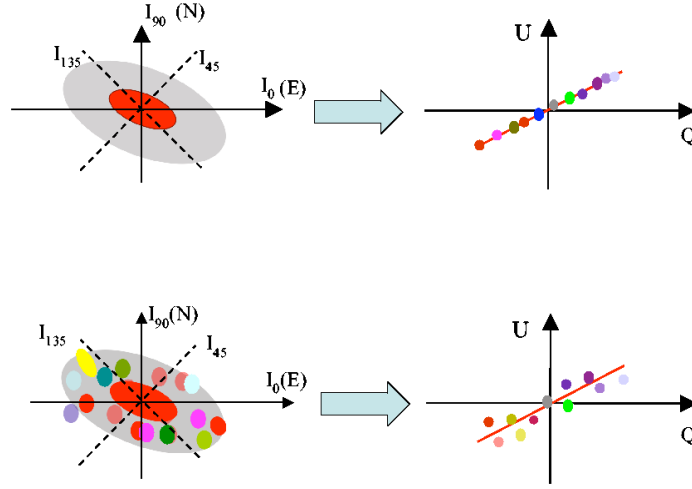


Figure 1: The top left illustrates a smooth, axisymmetric structure with the axis tilted at an arbitrary position angle on the sky. The directions denoted by I represent the measurement of the flux at the angles needed to construct the Q and U polarization components (§3.1). The resulting wavelength-dependent polarization amplitude plotted in the Q/U plane will follow a straight line, the dominant axis, as illustrated in the top right. Dots represent the polarization measured at different wavelengths. The lower left illustrates a case for which the axisymmetry is broken into “clumps” of different composition and optical depth. Clumps of high-opacity, absorbing material will block parts of the underlying, photosphere. This will induce wavelength-dependent geometry. The polarization distribution in the Q/U plane will in general no longer be along a straight line, as illustrated in the lower right. The basic axisymmetric geometry may still be evident, as illustrated, but the departure from axial symmetry caused by the “clumping” will yield a finite, and physically significant, distribution along the orthogonal axis. The Q/U diagrams on the upper and lower right represent spectropolarimetry Types D0 and D1, respectively, as defined in §3.6.

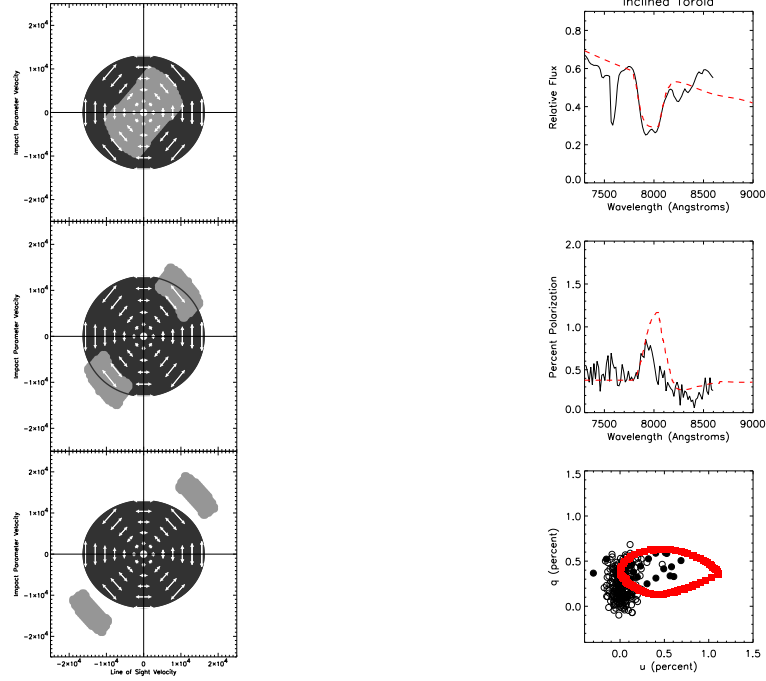


Figure 2: The left half shows velocity slices through an edge-on torus surrounding an ellipsoidal photosphere, both expanding homologously. This geometry breaks the axisymmetry. The torus has a strong absorption line that blocks the continuum emission from the photosphere. The geometry of the blocking region depends on the velocity slices through the structure and hence on the wavelength across the line profile. The arrows mark the photospheric polarization angle and amplitude. The three panels show decreasing blue shift. The right half shows the effect of the torus, now tilted both with respect to the line of sight and to the axis of the underlying ellipsoidal photosphere, on the total flux line feature, the polarization feature, and as depicted in the Q/U plane. The polarization is somewhat strong compared to the particular observations of the Type Ia supernova SN 2001el (§5.1.1), but the locus in the Q/U plane shows a loop that matches the observations rather well. From Kasen et al. (2003).

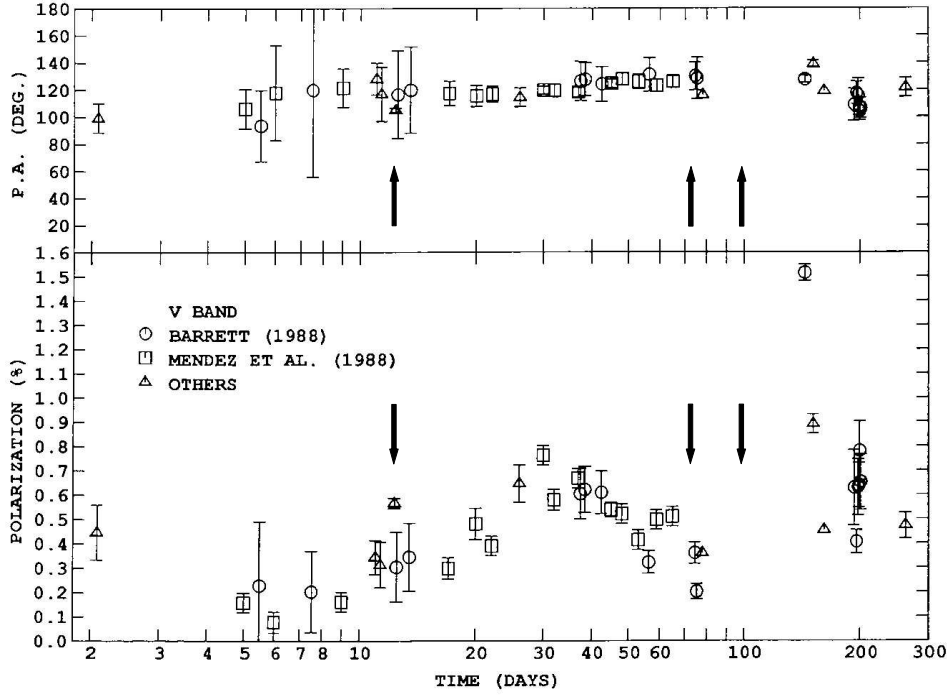


Figure 3: Evolution of the V-band polarization and associated polarization angle of SN 1987A from Jeffery (1991a). Note the near constancy of the polarization angle despite the variation in the amplitude of the broad band polarization. Vertical arrows indicate the epochs for which spectropolarimetry is presented in Figures 4 and 5.

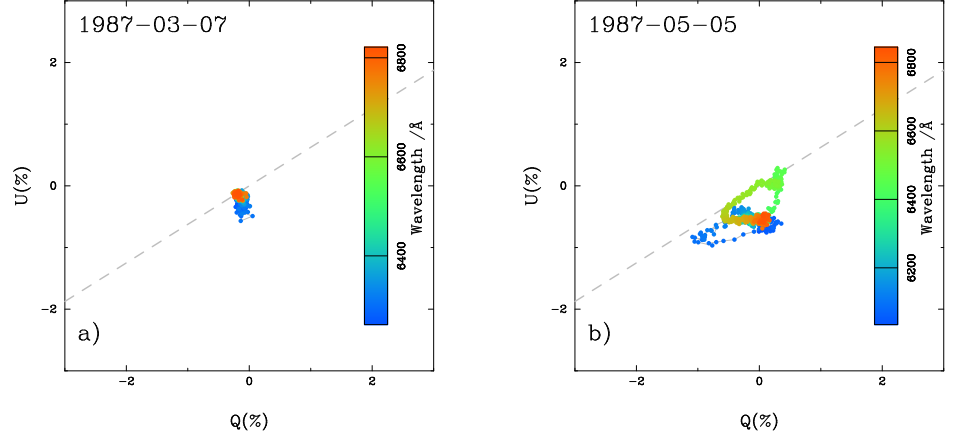


Figure 4: (Left Panel) $H\alpha$ and adjacent continuum in the Q/U plane for SN 1987A on March 7, 1987, about two weeks after the explosion. The data cluster near the origin with some small departure to negative U at a position angle of about 150° . (Right Panel) $H\alpha$ and adjacent continuum on May 5, 1987, near maximum light. The $H\alpha$ polarization has developed a distinct “loop” structure indicating significant departures from axisymmetry and bears little relation to the data of March 7. The solid line corresponds to the “speckle angle,” $\theta \sim 16^\circ$ (Meikle et al. 1987) in the negative quadrant and extrapolated into the positive quadrant as if there were an oblate counterpart as a guide to the eye. The data have been corrected for the ISP given by Méndez (1990; Jeffery 1991a). Adapted from Cropper et al. (1988).

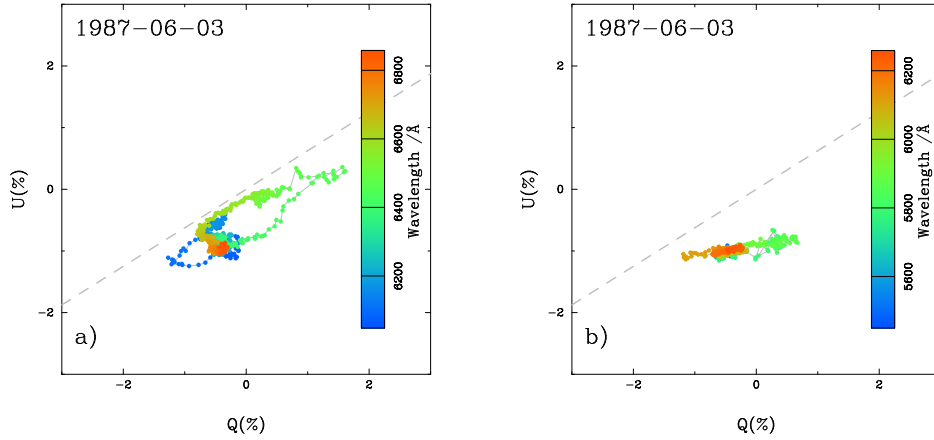


Figure 5: (Left Panel) $H\alpha$ and adjacent continuum on the Q/U plane for SN 1987A on June 28, 1987, as the fading from peak began. The “loop” structure is now especially prominent. (Right Panel) He I λ 5876 and adjacent continuum on June 28, 1987. The data at around 5600 and 6200 Å represent the continuum. The He I line shows a large excursion to $Q \sim 0.7\%$ at 5800 Å at absorption minimum. The data at $Q \sim -1.2\%$ at 6100 Å corresponds to the absorption minimum of the adjacent Ba II line. All these features fall closely along the same locus. The solid line corresponds to the “speckle angle,” $\chi \sim 16^\circ$ (Meikle et al. 1987) in the negative quadrant and extrapolated into the positive quadrant as if there were an oblate counterpart as a guide to the eye. The data have been corrected for the ISP given by Méndez (1990; Jeffery 1991a). Adapted from Cropper et al. (1988).

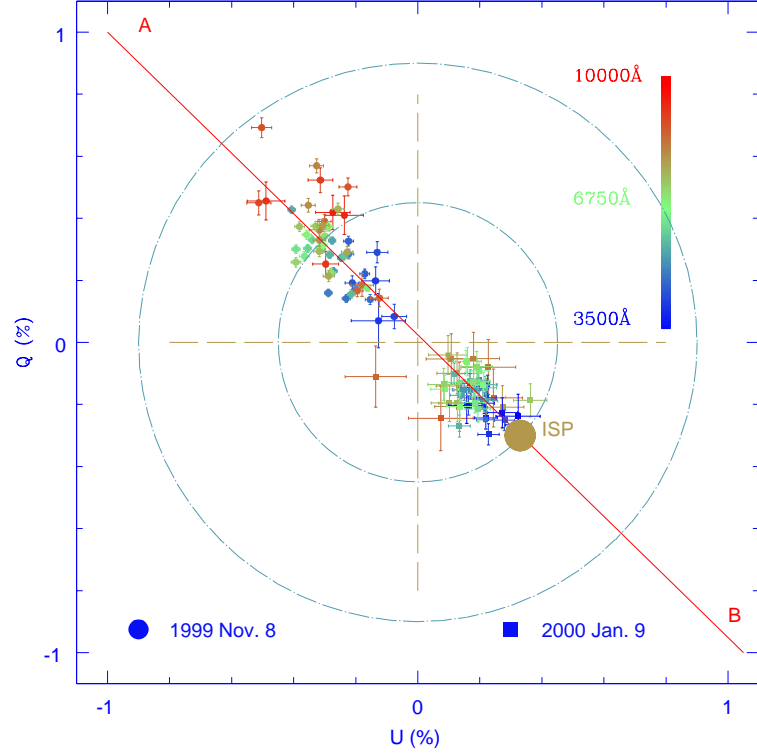


Figure 6: Polarimetry of the Type II SN 1999em. The wavelengths represented by different data points are color encoded. The 1999 2 Nov. data (clustered in the lower-right quadrant) corresponding to the early plateau are clearly separated from the 2000 9 Jan. data (clustered in the upper-left quadrant) on the late plateau, showing an increase in polarization with time. Line AB is the dominant axis. The circles are the upper limits to the interstellar polarization (measured with respect to the observed values $Q = 0$, $U = 0$) assuming $E(B-V)$ toward the supernova to be 0.05 (inner circle) and 0.1 (outer circle). The approximate location of the component due to interstellar dust is shown as a solid circle.

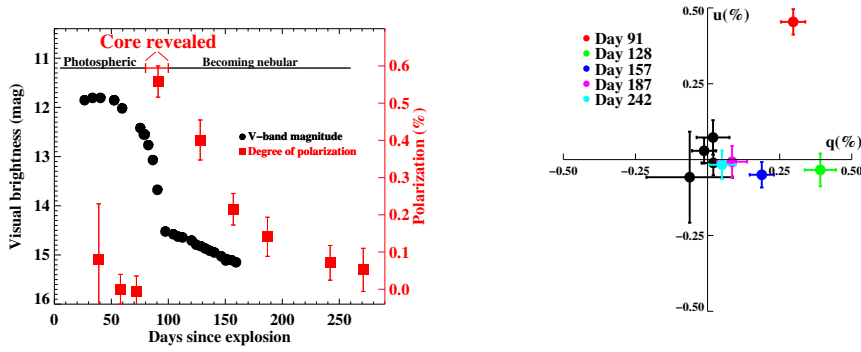


Figure 7: (Left Panel) Light curve and continuum polarization of SN 2004dj. The red points represent the median of the rotated Stokes parameter in the ISP-subtracted data over the spectral range 6800 - 8200 Å. From Leonard et al. (2006). (Right Panel) Evolution of SN 2004dj with time in the Q/U plane (courtesy D. Leonard).

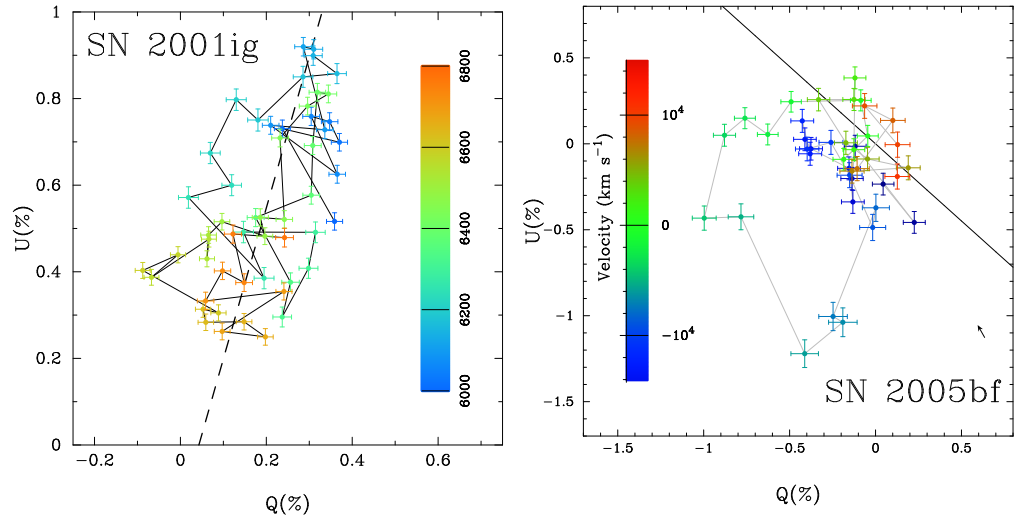


Figure 8: Q/U plane loops, corrected for the relevant ISP, of He I 6678Å/H α in the Type IIb SN 2001ig (Left Panel: Maund et al. 2007a) and He I 5876Å in the Type Ib/c SN 2005bf (Right Panel: Maund et al. 2007b). The loops are indicative of non-axisymmetric structure.

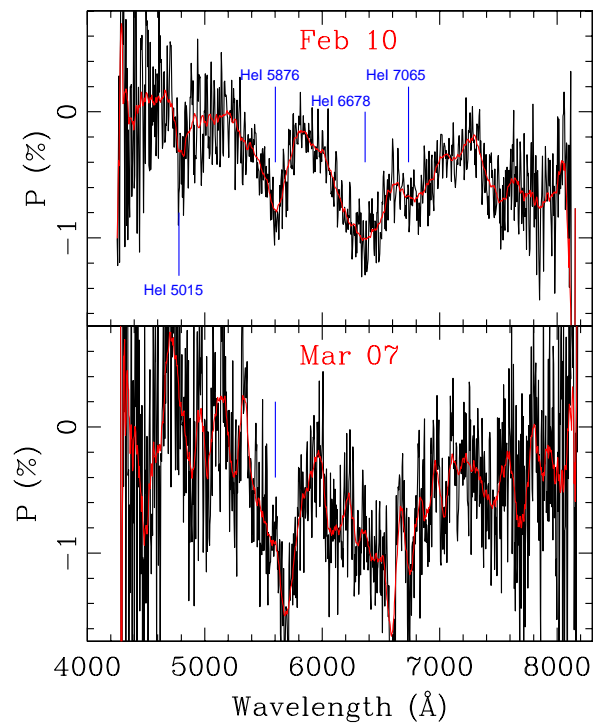


Figure 9: Polarization spectrum of Type Ic SN 1997X on 10 February and 7 March, 1997 approximately 5 and 30 days after maximum light. Note the prominent evidence for high velocity He I lines in the 10 February spectrum even though this event that was otherwise identified as being helium deficient.

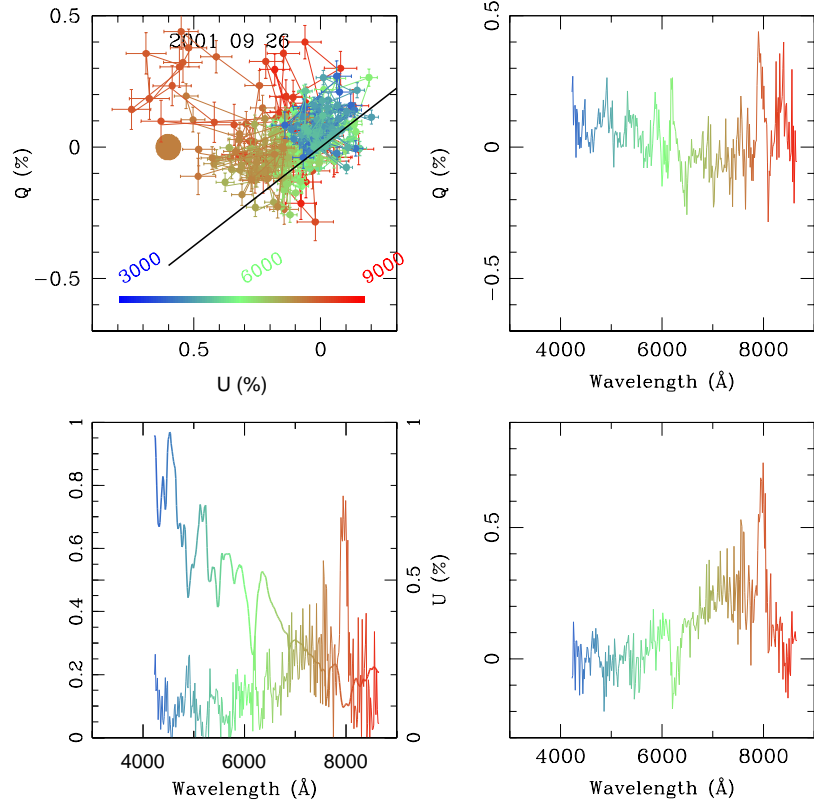


Figure 10: Spectropolarimetry of the Type Ia SN 2001el on 2001 Sept. 26, 7 days before maximum. The assumed interstellar polarization is shown as a solid dot in the Q/U plot (upper left). The straight line illustrates the dominant axis shifted to the origin of the Q/U plot. The Q (upper right) and U (lower right) spectra show conspicuously polarized spectral features. The flux spectrum is also given in the lower left panel as the line rising to the left. The lower left panel shows the correlations of the degree of polarization and the spectral features. The high-velocity Ca II IR feature is especially prominent at 8000 Å. The wavelength color code is presented at the bottom of the upper left panel. From Wang et al. (2003a).

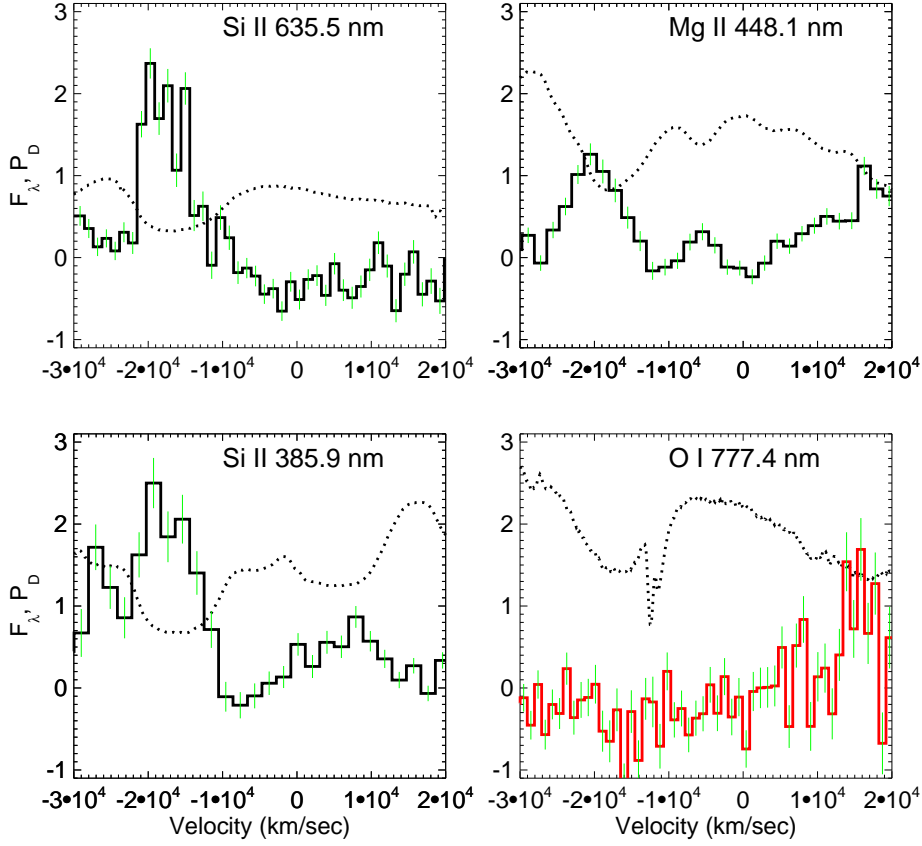


Figure 11: Polarized line features in SN 2004dt. Absorption features in the total flux spectrum and the polarization profiles along the dominant axis are given as a function of velocity for the lines of (clockwise from the upper left) Si II $\lambda 6355$, Mg II $\lambda 4471$, O I $\lambda 7774$, and Si II $\lambda 3859$. The dotted lines give the total flux profiles and the solid lines give the polarization. Note that there is significant polarization in all the lines except O I. From Wang et al. (2006).

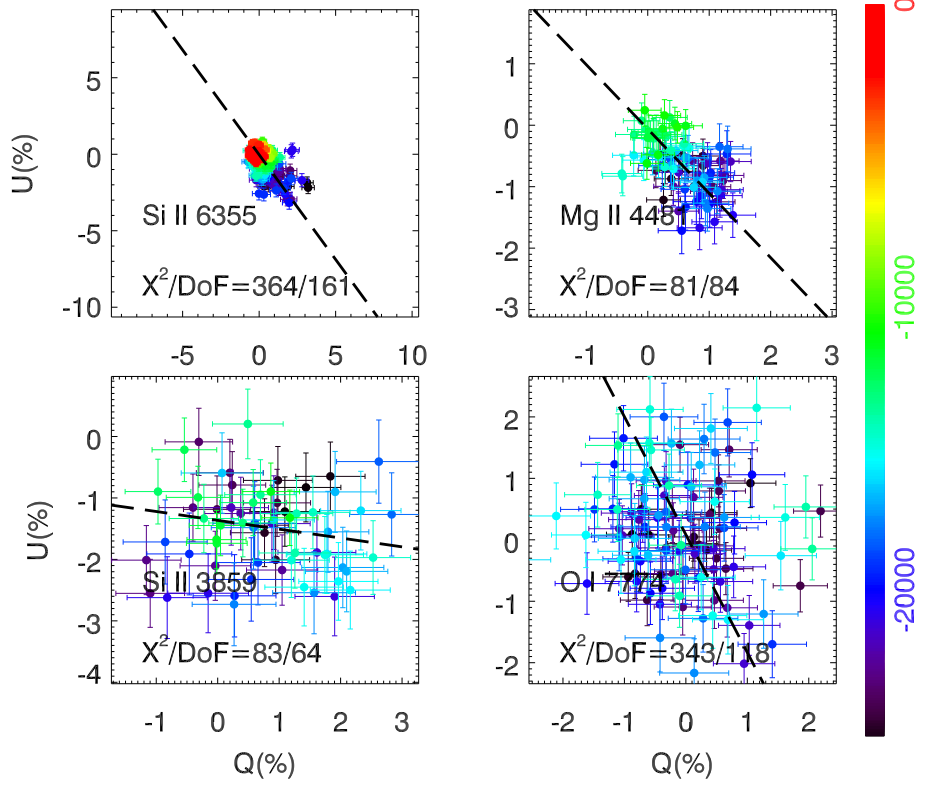


Figure 12: Q-U diagrams of the strongest lines in SN 2004dt and the corresponding linear fits given by the dashed lines. The ranges of the data points are from $-25,000$ to $-10,000$ km s^{-1} for these lines. The panels are for the lines of Si II $\lambda 6355$ (top left), Mg II $\lambda 4481$ (top right), O I $\lambda 7774$ (bottom right), and Si II $\lambda 3859$ (bottom left). Only the Mg II line is consistent with a straight line, indicating a simple axially symmetric geometry with no detectable clumping. From Wang et al. (2006).

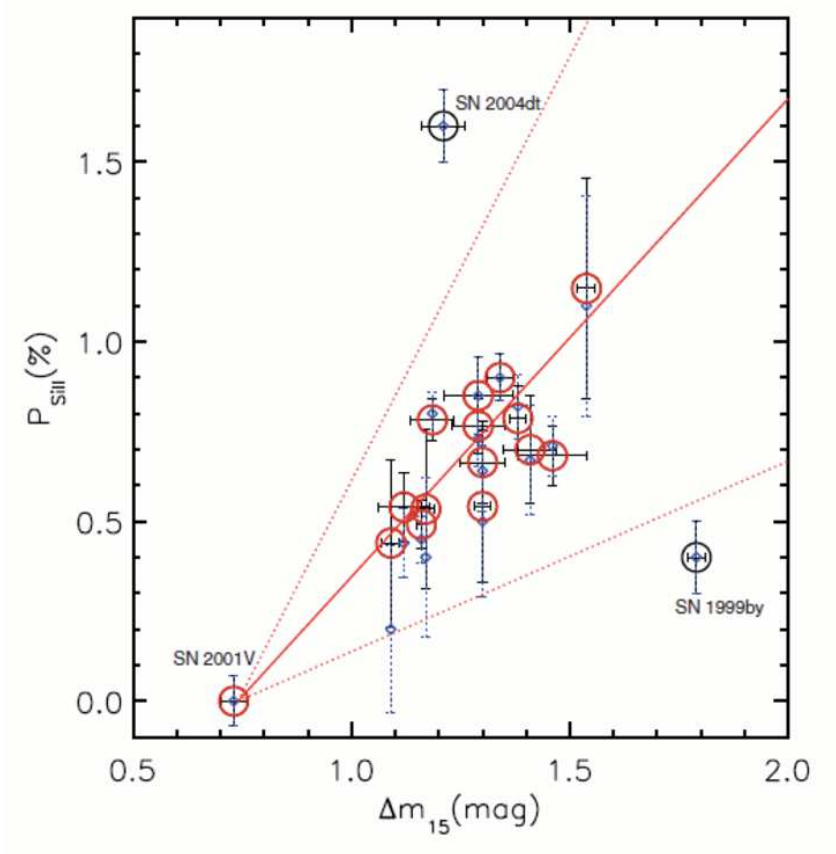


Figure 13: The correlation between the degree of polarization across the Si II $\lambda 6355$ line and the light curve decline rate, Δm_{15} , for a sample of 17 Type Ia supernovae corrected to 5 days after maximum. The linear fit represented by the straight line includes only spectroscopically normal supernovae shown as red open circles. The blue open circles show the highly polarized event SN 2004dt and the subluminal SN 1999by. The dotted lines illustrate the 1σ level of the intrinsic polarization distribution around the most likely value for the Monte Carlo simulation with 20 identical opaque clumps of Si II. From Wang, Baade, & Patat (2007).